Swansea University

MPhys Thesis

Theoretical Physics

Entanglement Entropy, Black Holes and Holography

Author:
Tom Bourton, 701329

22nd May 2015

Prifysgol Abertawe
Swansea University

Abstract

One of the most important concepts arising from string theory is the idea of Holography. Holography claims that degrees of freedom in a $(d+2)$ dimensional theory of quantum gravity is correspondent to a quantum field theory in $(d+1)$ dimensions. One of the most notable flavours of Holography is the AdS/CFT correspondence which argues that quantum gravity in $(d+2)$ dimensions can be completely described by degrees of freedom in $(d+1)$ dimensional conformal field theory living on the AdS boundary. The correspondence is made exact via equivalence of the AdS and CFT partition functions. Some principles of the AdS/CFT correspondence are demonstrated via relating fields in bulk AdS to CFT observables on the boundary. CFT entanglement entropy's are calculated via the AdS/CFT correspondence. The entanglement entropy gives a measure of how entangled (or how 'quantum') a given state $|\Psi\rangle$ is. Remarkably, the AdS/CFT correspondence provides a prescription to calculate large N CFT entanglement entropy's with weakly coupled classical gravity holographic duals on AdS space. The prescription relates minimal surfaces in AdS to CFT entanglement entropy's via a generalization of the Bekenstein-Hawking area law for black hole entropy. This area law is initially applied to a variety of static geometries and the possibility of interpreting a phase transition in minimal surfaces to that of a CFT confinement/deconfinement phase transition. The entanglement entropy prescription is then applied to dynamical systems, specifically in the effort of modelling, via Holographic techniques, a CFT undergoing a quantum quench, whereby a CFT undergoes a perturbation, bringing the system far from equilibrium and the entanglement entropy is used to study the evolution of the system as it returns to an equilibrium-like state. The holographic dual of the quench process is given in terms of a Vaidya geometry. Thermalisation times for quantum quenches for both CFT_2 and CFT_3 are numerically obtained which are found to be $t_T \simeq \frac{\ell}{2}$ and $t_T \simeq \frac{2\ell}{3}$ respectively.

Contents

Chapter 1

Introduction

Holography is an important property arising from string theory. It claims that degrees of freedom in a theory of quantum gravity in $(d+2)$ dimensions can be completely described by the degrees of freedom of a $(d+1)$ dimensional theory quantum field theory which is said to be the holographic dual to theory gravitational theory [31]. One of the most notable flavours of Holography is the AdS/CFT correspondence. The correspondence, originally proposed by Maldacenda [26] who claimed that there is correspondence between string theory on $AdS_5 \times \mathbf{S}^5$ and $\mathcal{N} = 4$ Yang-Mills. The AdS/CFT correspondence claims that degrees of freedom in $(d+2)$ quantum gravity on AdS can be completely described by degrees of freedom in $(d+1)$ dimensional conformal field theory and the conformal field theory is said to live on the AdS boundary $\partial(AdS)$.

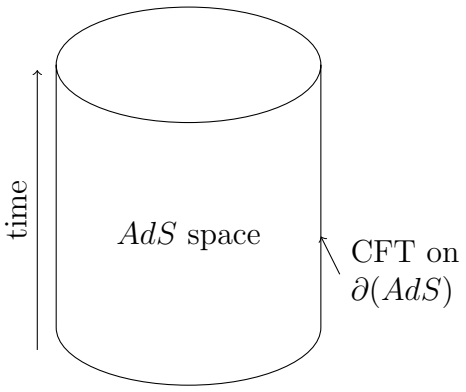

Figure 1.1: Pictorial representation of the AdS/CFT correspondence

Fig.(1.1) shows a simple pictorial representation of the correspondence. The hyperbolic AdS space can be built up of a "stack" of constant time slices to form a $d+2$-dimensional cylinder. The degrees of freedom of any given slice of AdS can be described by a conformal field theory on the $(d+1)$-dimensional AdS boundary $\partial(AdS)$.

A hint towards this holographic correspondence between quantum gravity and quantum field theory can be seen in Bekenstein-Hawking entropy [18, 6] which says that entropy of a black hole is proportional not to its volume but to the area of its horizon

$$S_{BH} = \frac{Area_{horizon}}{4G_N}, \tag{1.1}$$

where G_N is Newton's constant. Following from this relation it was proposed in [31] that the entanglement entropy may be obtained using holography and a generalisation of (1.1). The entanglement entropy S_A of a region A of a given QFT is defined as the von Neumann entropy obtained by tracing out degrees of freedom not contained in A. We denote the region containing the rest of the system is given by B. The entanglement entropy may be considered as counting degrees of freedom which cannot be accessed by an observer in region A when tracing out the region B. Then the entanglement entropy is given by the area law [31]

$$S_A = \frac{Area(\gamma_A)}{4G_N^{(d+2)}} \tag{1.2}$$

where, for static non-time dependent backgrounds, the manifold γ_A is a d-dimensional minimal surface extending into AdS_{d+2} from the region A on the boundary.

In sections (2) and (3) some definitions concerning density matrices and entanglement entropy respectively are given. In section (4) some aspects of the AdS/CFT correspondence are given, including calculations of CFT two-point functions and conserved currents which can be found in [34]. In section (5) some entanglement entropy calculations are performed via holographic methods using equation (1.2). Then in section (6) the holographic relation between black holes and thermal CFT's are given and the entanglement entropy for a thermal CFT_2 is calculated. In section (7) the area law proposal (1.2) is demonstrated for time-dependent backgrounds, focusing specifically on the evolution of the entanglement entropy of both a CFT_2 and CFT_3 undergoing a quantum quenches using the AdS/CFT correspondence where the holographic dual is given by a Vaidya geometry [1].

Chapter 2

Pure/Mixed States & Density Matrices

2.1 Pure States & Density Matrices

A pure quantum state $|\psi\rangle$ acting on a Hilbert Space can be described by an ensemble of orthogonal state vectors $\{|n\rangle\}$ such that $|\psi\rangle$ can be expanded in terms of a Hermitian operator H

$$|\psi\rangle = \sum_n c_n |n\rangle, \quad \text{where} \quad H|n\rangle = \lambda_n |n\rangle . \tag{2.1}$$

Thus $(c_n)^2$ is interpreted as the probability to measure eigenvalue λ_n. This probability can also be described as a fraction of the number of times the eigenvalue λ_n is measured with respect to the number of measurements taken $(c_n)^2 = \frac{N_n}{N}$.
We may define a density matrix $\rho \equiv |\psi\rangle \langle\psi|$ for the pure system, for a pure system the density matrix has the following properties:

$$\rho^2 = |\psi\rangle \langle\psi|\psi\rangle \langle\psi| = \rho \tag{2.2}$$
$$\rho^\dagger = \rho \tag{2.3}$$
$$\mathrm{Tr}(\rho) = 1 \tag{2.4}$$
$$\rho \geq 0. \tag{2.5}$$

Expectation values of observables may be calculated from the density matrix

$$\begin{aligned} \langle H \rangle_\rho &= \mathrm{Tr}\left(\rho H\right) \\ &= \sum_n \langle n|\psi\rangle \langle\psi|H|n\rangle \\ &= \langle\psi|H|\psi\rangle . \end{aligned} \tag{2.6}$$

2.2 Mixed States

A pure state is not the most general state that can be constructed, a general state may be entangled and mixed with other states, thus pure state vectors can no longer adequately describe the statistical mixing of states. A mixed state can be thought of as a collection of **N** pure states $\{|\psi_i\rangle\}$ with a probability to find an individual

subsystem in the state $|\psi_i\rangle$ given by $p_i = \frac{\mathbf{N}_i}{\mathbf{N}}$. The system can be expressed by a density matrix, defined as a weighted sum of pure state density matrices

$$\rho^{mix} = \sum_i p_i \left|\psi_i\right\rangle \left\langle\psi_i\right| = \sum_i p_i \rho_i^{pure}. \tag{2.7}$$

For a mixed state (2.2) no longer holds, now

$$\rho_{mix}^2 = \sum_i p_i^2 \left|\psi_i\right\rangle \left\langle\psi_i\right| \neq \rho_{mix}. \tag{2.8}$$

The quantity $\mathrm{Tr}(\rho^2)$ is time independent which can be shown by applying the unitary time evolution operator $U = e^{-iHt}$

$$\mathrm{Tr}(\rho(t_0)^2) = \mathrm{Tr}(U\rho\left(t_0\right)U^\dagger U\rho\left(t_0\right)U^\dagger) = \mathrm{Tr}(\rho\left(t_0\right)^2) \tag{2.9}$$

The expectation value of an operator H may be calculated by taking the trace of the density matrix multiplied with the operator

$$\left\langle H\right\rangle_{\rho_{mix}} = \mathrm{Tr}\left(\rho_{mix}H\right) = \sum_i p_i \left\langle\psi_i|H|\psi_i\right\rangle. \tag{2.10}$$

Chapter 3

Entanglement Entropy

3.1 Quantum Entanglement

A quantum state is said to be entangled if it cannot be written as a direct product of states from the subsystem Hilbert Spaces. Loosely speaking, it says that if we have a pair of entangled states $|\psi\rangle = |\Psi_A \bigotimes \Psi_B\rangle$ then performing a measurement on system A collapses the wave function $|\psi\rangle$. This implies that measurements on system A can affect system B, thus systems A and B are entangled.

3.2 Entanglement Entropy

It is useful to be able to quantify and measure how strongly entangled quantum states are. Such a measurement must vanish for a pure, non-entangled state and must be independent of basis. An example of such a measure is known as the Entanglement Entropy which is given by

$$S(\rho) = -Tr\left(\rho \log \rho\right). \tag{3.1}$$

For example, if two subsystems A & B are prepared with Hilbert spaces H_A & H_B respectively, such that a general quantum state is of the form $|\psi\rangle \in H_A \bigotimes H_B$. Then a density matrix for the full system can be written as

$$\rho = |\psi\rangle \langle\psi| \tag{3.2}$$

Now it is possible to extract a measure for how strongly system A is entangled with system B by constructing a reduced density matrix ρ_A for system A by "tracing out" system B. The reduced density matrix ρ_A for system A is then given by

$$\rho_A = Tr_B(\rho) = \sum_j |j_B\rangle(|\psi\rangle \langle\psi|) \langle j_B| \tag{3.3}$$

where the sum over j sums over all possible states of subsystem B. Then the measure of Entanglement of system A with system B is given by

$$S(\rho_A) = -Tr\left(\rho_A \log \rho_A\right) \tag{3.4}$$

and since $\mathrm{Tr}(M) = \sum_j \lambda_j$ for any matrix M

$$S(\rho_A) = -\sum_j p_j \log p_j. \tag{3.5}$$

As an example, consider a two spin quantum system in a pure state divided into two subsystems A and B and we wish to calculate the entanglement entropy of A [27]. If we first consider a non-entangled state $|\psi>=|\uparrow_A\uparrow_B>$ which, in the representation $|\uparrow_A>=\begin{pmatrix}1\\0\end{pmatrix}$, $|\downarrow_A>=\begin{pmatrix}0\\1\end{pmatrix}$, then the reduced density matrix for the subsystem A is

$$\rho_A = |\uparrow_A><\uparrow_A| = \begin{pmatrix}1 & 0\\ 0 & 0\end{pmatrix}. \tag{3.6}$$

Applying (3.5) gives the entanglement entropy

$$S(\rho_A) = -\log(1) = 0, \tag{3.7}$$

so the entanglement entropy vanishes, as expected, for a non-entangled state. For an entangled state $|\psi>=\frac{1}{\sqrt{2}}(|\uparrow_A\uparrow_B> + |\downarrow_A\downarrow_B>)$

$$\rho_A = \frac{1}{2}(|\uparrow_A><\uparrow_A| + |\downarrow_A><\downarrow_A|) = \frac{1}{2}\begin{pmatrix}1 & 0\\ 0 & 1\end{pmatrix}, \tag{3.8}$$

giving the entanglement entropy

$$S(\rho_A) = -\log\left(\frac{1}{2}\right) \neq 0 \tag{3.9}$$

so the entanglement entropy for an entangled state in non-zero as expected.

Chapter 4

The AdS/CFT Correspondence

4.1 Holography and the AdS/CFT Correspondence

We wish to use the entanglement entropy to probe strongly coupled quantum field theories. Calculation directly from the field theory requires the taking of traces of density matrices which is, in general very complex, thus we require a more simple method for calculating QFT entanglement entropy's.

One such tool which may be used is Holography. Holography describes a duality relating a theory on a manifold M to a boundary theory on ∂M, thus the boundary theory appears as a "hologram" of which completely describes all degrees of freedom in bulk theory. Holography, and more specifically the Gauge/Gravity duality says that for a QFT at strong coupling there exists a dual theory of quantum gravity at weak coupling in one higher dimension. This gives us a powerful tool as gravitational theories at weak coupling are well understood and calculations are generally less complex than those of gauge theory. One of the most well understood flavours of Holography is the Anti-de Sitter(AdS)/Conformal Field Theory(CFT) correspondence.

The AdS/CFT Correspondence was conjectured by Juan Maldacena [26], who proposed that there is a duality between string theory on $AdS_5 \times \mathbf{S}^5$ and $\mathcal{N} = 4$ $SU(N)$ supersymmetric Yang-Mills theory in $d = 3 + 1$ dimensions. In general the AdS/CFT correspondence says that for a CFT_{d+1} there is a dual to a gravitational theory in AdS_{d+2} space, where $d + 2$ represents AdS space with $d + 1$ spatial dimensions and 1 time-like dimension. The boundary of AdS space is conformally equivalent to Minkowski space locally, in the neighbourhood of any point on the boundary. Therefore it can be said that the CFT_{d+1} lives on the boundary of a AdS_{d+2} manifold and the correspondence tells us that the degrees of freedom in the bulk of AdS are represented by degrees of freedom in the CFT dual on the boundary. Some arguments which point to the existence such as comparing the degrees of freedom of the two dual theories and symmetry matching are given below.

4.2 Comparing Degrees of Freedom

It is possible to compare the number of degrees of freedom for the two theories, for a CFT on $\mathbb{R}^{1,d}$. The CFT first must be confined to a finite spatial region L^d (to act as a IR cutoff) and imposing a UV cutoff ϵ in d spatial directions. For a $SU(N)$ conformal gauge theory, the number of degrees of freedom per site is $\propto N^2$ then the

total number of degrees of freedom in the theory is given by

$$N_{dof}^{CFT} = N^2 \left(\frac{L}{\epsilon}\right)^d. \tag{4.1}$$

In AdS_{d+2}, or indeed any gravitational theory, the upper bound on number of degrees of freedom given by the entropy of the black hole which fills the entire space. The No-hair conjecture tells us that black hole solutions to Einstein's equations can be completely described by the black hole's electric charge E, mass M and angular momentum J [28] and therefore the black hole entropy represents the maximal entropy due to the large number of microstates that can be filled that result in a black hole with the same three classical No-hair parameters. The entropy of a black hole is given by the Bekenstein-Hawking Entropy (4.2) which tells us that the entropy of the black hole is proportional to area of its horizon [18, 6]

$$S_{BH} = \frac{Area_{horizon}}{4G_N^{(d+2)}}. \tag{4.2}$$

$$Area_{horizon} = \int_{R^d} \sqrt{h} d^d x = \left(\frac{R}{\epsilon}\right)^d L^d, \tag{4.3}$$

where h is the determinant of the induced metric on the d dimensional surface of the black hole horizon, ϵ is a UV cutoff and L^d is the finite volume occupied by the system. The total number of degrees of freedom in the gravity theory is then given by the ratio of the Plank length and the total size of the system

$$N_{dof}^{AdS} = \frac{1}{4G_N^{(d)}} \left(\frac{R}{\epsilon}\right)^d = \frac{1}{4} \left(\frac{R}{\epsilon}\right)^d \left(\frac{L}{l_p}\right)^d. \tag{4.4}$$

Thus for the limit that N is large, the CFT has a classical gravity dual as classical gravity $\Rightarrow \frac{L}{l_p} \gg 1$.

4.3 Conformal Group & AdS

If there exists a dual between a CFT in $d+1$ dimensions and AdS space in $d+2$ dimensions then we expect to find a symmetry transformation which leaves both theories invariant, it can be shown that this is true for for the case of the AdS/CFT correspondence.

A Conformal Field Theory(CFT) is a type of Quantum Field Theory which is invariant under conformal transformations and appears at a fixed point in the renormalization group flow. A conformal transformation is a transformation that preserves only the angles within the space. $d+1$ dimensional Minkowski space, $\mathbb{R}^{1,d}$, has isometry group $SO(1,d)$ (the Poincaré Group). The space of conformal transformations forms a finite group spanned by $SO(2,d+1)$. For a CFT_{1+1} such transformations are made up by [23]

$$\begin{aligned}
\text{Translations}: &\quad x^\mu \to x^\mu + a^\mu \\
\text{Rotations}: &\quad x^\mu \to \omega^\nu_\mu x^\nu \\
\text{Boosts}: &\quad x^\mu \to \lambda x^\mu \\
\text{Special Conformal Transformations}: &\quad x^\mu \to \frac{x^\mu + b^\mu x^2}{1 + 2b.x + b^2 x^2}.
\end{aligned}$$

A general AdS coordinate system in $d+2$ dimensions can be written as

$$\chi_1{}^2 + \chi_2{}^2 + ... + \chi_{d+1}{}^2 - \chi_{d+2}{}^2 - \chi_{d+3}{}^2 = -R^2, \tag{4.5}$$

which has isometry group $SO(2,d+1)$ and is manifestly invariant under a $SO(2,d+1)$ group transformation. Therefore, the group $SO(2,d+1)$ acts upon AdS_{d+2} as a group of ordinary symmetries and it acts upon a CFT_{d+1} as a group of conformal symmetries. The boundary of AdS_{d+2} can be shown to be a copy of Minkowski space $\mathbb{R}^{1,d}$ as can be seen from the half space Poincaré patch metric

$$ds^2 = \frac{1}{z^2}(dz^2 - dt^2 + \sum_i dx_i^2) \tag{4.6}$$

in the limit $z \to 0$ the metric becomes conformally equivalent to Minkowski space $ds^2 = (-dt^2 + \sum_i dx_i^2)$. This implies that we have two ways in which to build a physical theory with $SO(2,d+1)$ symmetry: a quantum field theory on AdS_{d+2} or a conformal field theory on $\mathbb{R}^{1,d}$.

4.4 Calculating CFT observables from the AdS/CFT correspondence

To further demonstrate this holographic principle, following the prescription by Witten [34], boundary field theory observables can be calculated using the AdS/CFT correspondence. The holographic principle tells us that boundary CFT correlation functions are given by the asymptotic behaviour at infinity of the string/supergravity action. In the large N limit we may approximate to a supergravity action as the string coupling $g_{st} \propto g_{YM}^2$, with g_{YM} the Yang-Mills coupling with gauge group $SU(N)$. We also have the AdS radius $R \propto (g_{YM}^2 N)^{1/4}$ therefore $\frac{R^4}{g_{st}} \propto N$, therefore we deduce that large-N Yang-Mills corresponds to small g_{st}. In this limit "stringy" corrections are suppressed and we may use a supergravity approximation. The supergravity action $S_{SG}(\phi, A_\mu, g_{\mu\nu}, B_{\mu\nu})$ may contain scalars (ϕ), gauge fields (A_μ) and rank-two symmetric ($g_{\mu\nu}$) and anti-symmetric tensor ($B_{\mu\nu}$) fields [37].

We wish to compute correlation functions $\langle \mathcal{O}(x_1)\mathcal{O}(x_2)...\mathcal{O}(x_n)\rangle$ for $x_1, x_2, ..., x_n \in \mathbf{S}^d$. Calculating these quantities for arbitrary n using conventional methods from field theory would inevitably result in difficulty in renormalization The AdS/CFT correspondence precisely says that

$$Z_{CFT} = Z_{SG}. \tag{4.7}$$

Setting

$$Z_{SG} = \exp(-S_{SG}(g)), \tag{4.8}$$

where g is a solution of Einstein's equations with the required boundary behaviour. For a massless scalar ϕ in AdS_{d+1} with boundary value ϕ_0. Assuming in AdS/CFT the boundary value ϕ_0 will couple to a conformal field $\mathcal{O}$ with a coupling $\int_{S_d} \phi_0 \mathcal{O}$, ϕ_0 has conformal weight 0, therefore $\mathcal{O}$ has conformal dimension d. Then

$$Z_{SG}(\phi_0) = \exp(-S_{SG}(\phi)) \tag{4.9}$$

then the relation between the CFT on the boundary to AdS is

$$\left\langle \exp\left(\int_{S_d} \phi_0 \mathcal{O}\right)\right\rangle_{CFT} = Z_{SG}(\phi_0) \tag{4.10}$$

4.4.1 Massless scalar in AdS

In the following sections, for simplicity the CFT dimension is denoted by d and AdS dimensionality is therefore $d+1$. The calculations will be performed using the Euclidean upper half Poincaré patch metric of AdS space with positive-definite signature. In $d+1$ dimensions AdS can be described by the ball $\mathbf{B}_{d+1}$ in this representation the boundary is a copy of $\mathbb{R}^d$ located at $x_0 = 0$ together with a single point P located at $x_0 = \infty$, thus the AdS_{d+1} boundary in this representation is $\mathbf{S}_d$, obtained by the conformal compactification of $\mathbb{R}^d$ by adding in a point at infinity

$$ds^2 = \frac{1}{x_0^2}\left(dx_0^2 + \sum_{i=1}^{d} dx_i^2\right). \tag{4.11}$$

For a massless scalar ϕ in AdS with action

$$I(\phi) = \frac{1}{2}\int_{B_{d+1}} d^{d+1}y\sqrt{g}|d\phi|^2. \tag{4.12}$$

Which obeys the Laplace equation

$$D_i D^i \phi = 0 \tag{4.13}$$

Take the boundary value ϕ_0 to be the value of ϕ at the boundary $x_0 = \infty$ and is a source for a field $\mathcal{O}$ which is the boundary field theory. We wish to solve for ϕ in terms of only boundary terms and then evaluate the action (4.12) in an aim to compute 2-point function for the field $\mathcal{O}$ on the boundary.

The point P is taken to be a point on the boundary at $x_0 = \infty$. The boundary conditions and metric has translational invariance in the x_i directions. We look for a Green's function solution G. Green's functions have the property

$$D_i D^i G(x, x') = \delta(x - x') \tag{4.14}$$

and for a function $v(x)$ with a classical source $u(x)$ at the boundary

$$v(x) = \int u(x')G(x, x')dx'. \tag{4.15}$$

The Laplace-Beltrami equation for a metric $g_{\mu\nu}$ is given by

$$D_i D^i \phi = \frac{1}{\sqrt{g}}\partial_\mu\left(\sqrt{g}g^{\mu\nu}\partial_\nu\right)\phi = 0 \tag{4.16}$$

where $g = \det(g_{\mu\nu})$ and $g^{\mu\nu}$ is the inverse metric tensor. Therefore the Laplace equation with metric (4.11) for the Greens function $G(x_0)$ reads

$$x_0^{(d+1)}\frac{\partial}{\partial x_0}\left(x_0^{-(d+1)}x_0^2\frac{\partial}{\partial x_0}G(x_0)\right) = 0, \tag{4.17}$$

$$\frac{\partial}{\partial x_0}\left(x_0^{-d+1}\frac{\partial}{\partial x_0}G(x_0)\right) = 0. \tag{4.18}$$

This is solved with $G(x_0) = A + Bx_0^d$ with A and B arbitrary constants, we require $G(x_0)$ to vanish at $x_0 = 0$, therefore take $A = 0$. As $x_0 \to \infty$, $G(x_0) \to \infty$ but

we may make a $SO(1,d+1)$ conformal transformation which allows us to map any point at infinity to a finite point. The point P can be mapped to the origin with the transformation

$$x_i \to \frac{x_i}{x_0^2 + \sum_{j=1}^d x_j^2}. \tag{4.19}$$

Under this transformation $G(x_0)$ transforms as

$$G(x) \to B\frac{x_0^d}{(x_0^2 + \sum_{j=1}^d x_j^2)^d}. \tag{4.20}$$

Then $\phi(x_0, x_i)$ is given by

$$\phi(x_0, x_i) = \int \phi_0(x_i')G(x_i, x_i')d\underline{x}' \tag{4.21}$$

$$= B\int \phi_0(x_i')\frac{x_0^d}{(x_0^2 + |\underline{x} - \underline{x}'|^2)^d}d\underline{x}' \tag{4.22}$$

where $|\underline{x}|^2 = \sum_{j=1}^d x_j^2$. By applying integration by parts the action (4.12) may be written as

$$I(\phi) = \frac{1}{2}\int_{\mathbf{B}_{d+1}} d^{d+1}y\sqrt{g}d(\phi d\phi) + \int_{\mathbf{B}_{d+1}} d^{d+1}y\sqrt{g}\phi dd\phi \tag{4.23}$$

$$= \frac{1}{2}\int_{\mathbf{S}_d} d^d y x_0^{-(d+1)}(\phi d\phi)\hat{n}_i \tag{4.24}$$

where the second term of (4.23) vanishes due to the equation of motion and the exterior derivative squared $d^2 = 0$ (4.13).

$$I(\phi) = \frac{1}{2}\lim_{\epsilon\to 0}\int_{T_\epsilon} d\underline{x}x_0^{-(d+1)}(\phi g^{ij}\nabla_j\phi)\hat{n}_i = \frac{1}{2}\lim_{\epsilon\to 0}\int_{T_\epsilon} d\underline{x}x_0^{-d}\phi(\underline{\hat{n}}.\underline{\nabla})\phi, \tag{4.25}$$

where $\hat{n}$ is a normal vector pointing perpendicular to the surface T_ϵ satisfying $g_{\mu\nu}n^\mu n^\nu = 1$. Therefore $\underline{\hat{n}}.\underline{\nabla}\phi = x_0(\frac{\partial\phi}{\partial x_0})$. Following (4.22) for $x_0 \to 0$ we acquire

$$\frac{\partial\phi}{\partial x_0} \approx dBx_0^{d-1}\int d\underline{x}'\frac{\phi_0(x_i')}{|\underline{x} - \underline{x}'|^{2d}} + O(x_0^{d+1}). \tag{4.26}$$

Subbing in to (4.25) and recalling that for $x_0 = \epsilon \to 0$, $\phi \to \phi_0$

$$I(\phi) \approx \frac{Bd}{2}\int d\underline{x}d\underline{x}'x_0^{-d}\phi_0(\underline{x})\frac{x_0^d}{|\underline{x} - \underline{x}'|^{2d}}\phi_0(\underline{x}') \tag{4.27}$$

$$= \frac{Bd}{2}\int d\underline{x}d\underline{x}'\frac{\phi_0(\underline{x})\phi_0(\underline{x}')}{|\underline{x} - \underline{x}'|^{2d}} \tag{4.28}$$

This is of the form of a two-point function $\langle\mathcal{O}(\underline{x})\mathcal{O}(\underline{x}')\rangle$ of a conformal field with conformal dimension d [37, 34]. We have calculated the two point function for a conformal field $\mathcal{O}$ on the boundary by evaluating the Supergravity AdS action containing a massless scalar field in the bulk.

4.4.2 Gauge Field in AdS

We can perform an analogous exercise for the case of a free gauge theory with gauge group $U(1)$ on the metric (4.11). We look for a one form solution A, i.e. the field is a vector field that carries one Lorentz index, $A = f(x_0)dx^i$ for a fixed $1 \leq i \leq d$. We must solve for Maxwell's equations

$$d(*F) = d(*dA) = 0. \tag{4.29}$$

With action

$$I(A) = \frac{1}{2}\int_{B_{d+1}} F \wedge *F. \tag{4.30}$$

The two form dA is given by

$$dA = \frac{\partial f(x_0)}{\partial x_\mu} dx^\mu \wedge dx^i = \frac{\partial f(x_0)}{\partial x_0} dx^0 \wedge dx^i. \tag{4.31}$$

Which gives the Hodge dual, which takes a k-form to a $(d-k)$-form, in this case taking the 2-form dA to the $d-2$-form

$$*dA = \frac{1}{2!}\epsilon_{i_1,i_2\ldots i_{d-2},j_1,j_2}\sqrt{g}g^{j_1 0}g^{j_2 i}f'(x_0)dx_0 \wedge dx_i \tag{4.32}$$

$$= \frac{(-1)^i}{2!}\sqrt{g}x_0^4 f'(x_0)dx^1 \wedge dx^2 \ldots \widehat{dx^i} \ldots \wedge dx^d \tag{4.33}$$

$$= \frac{(-1)^i}{2!}x_0^{-d+3} f'(x_0)dx^1 \wedge dx^2 \ldots \widehat{dx^i} \ldots \wedge dx^d \tag{4.34}$$

where $\widehat{dx^i}$ means that dx^i is omitted from the wedge product. The factor $(-1)^i$ comes from "anti-commuting" dx^i through the wedge product $(i-1)$ times using $dx^\mu \wedge dx^\nu = -dx^\nu \wedge dx^\mu$. Maxwell's equations (4.29) gives

$$d(*dA) = \frac{(-1)^i}{2!}\frac{\partial}{\partial x_\mu}\left(x_0^{-d+3}f'(x_0)\right)dx^\mu \wedge dx^2 \ldots \widehat{dx^i} \ldots \wedge dx^d \tag{4.35}$$

$$= \frac{(-1)^i}{2!}\frac{\partial}{\partial x_0}\left(x_0^{-d+3}f'(x_0)\right)dx^0 \wedge dx^2 \ldots \widehat{dx^i} \ldots \wedge dx^d. \tag{4.36}$$

To satisfy (4.29) we must pick $f(x_0)$ such that $\frac{\partial}{\partial x_0}\left(x_0^{-d+3}f'(x_0)\right) = 0$, this gives $f''(x_0) = x_0^1(d-3)f'(x_0)$ this gives $f(x_0) = Bx_0^{d-2}$ with B an undetermined constant which we may pick to be $B = \frac{d-1}{d-2}$, giving

$$A = \frac{d-1}{d-2}x_0^{d-2}dx^i. \tag{4.37}$$

As for the massless scalar, A diverges at the boundary $x_0 \to \infty$ which we may resolve by performing the transformation (4.19) giving

$$A = \frac{d-1}{d-2}\left(\frac{x_0}{x_0^2 + |\underline{x}^2|}\right)^{d-2} d\left(\frac{x^i}{x_0^2 + |\underline{x}|^2}\right) \tag{4.38}$$

$$= \frac{d-1}{d-2}\frac{x_0^{d-2}}{\left(x_0^2 + |\underline{x}^2|\right)^{d-1}}\left(dx_i - \frac{2x_i^2 dx_i}{x_0^2 + |\underline{x}^2|} - \frac{2x_0 x_i dx_0}{x_0^2 + |\underline{x}^2|}\right). \tag{4.39}$$

Due to the gauge freedom in A we may make a gauge transformation, as Maxwell's equations (4.29) are clearly invariant up to the adding of a term of the form of an exterior derivative of a scalar 0-form f to A (as $d(df) = 0$ by definition). Therefore we may add to (4.39) a term of the form $d(f)$

$$d(f) = -\frac{1}{d-2} d\left(\frac{x_0^{d-2} x_i}{(x_0^2 + |\underline{x}|^2)^{d-1}}\right) \tag{4.40}$$

$$= -\frac{x_0^{d-2}}{(x_0^2 + |\underline{x}|^2)^{d-1}} \left(\frac{x_i dx_0}{x_0} + \frac{dx_i}{(d-2)} - \frac{(d-1)}{(d-2)} \frac{2x_i^2 dx_i}{(x_0^2 + |\underline{x}^2|)} - \frac{(d-1)}{(d-2)} \frac{2x_0 x_i dx_0}{(x_0^2 + |\underline{x}^2|)}\right). \tag{4.41}$$

Adding (4.39) and (4.41) we obtain

$$A = \frac{x_0^{d-2}}{(x_0^2 + |\underline{x}|^2)^{d-1}} \left(dx_i - \frac{x_i dx_0}{x_0}\right). \tag{4.42}$$

If we want a solution of Maxwell's equations at $x_0 = 0$ coinciding with the source $A_0 = \sum_{i=1}^{d} a_i dx^i$ on the boundary, then using the Green's function (4.42) we have

$$A(x_0, \underline{x}) = \int d\underline{x}' A(\underline{x}, \underline{x}') A_0(\underline{x}') \tag{4.43}$$

$$= x_0^{d-2} \int d\underline{x}' \frac{a_i(\underline{x}') dx^i}{(x_0^2 + |\underline{x} - \underline{x}'|^2)^{d-1}} - x_0^{d-3} dx_0 \int d\underline{x}' \frac{a_i(\underline{x}')(x^i - x'^i)}{(x_0^2 + |\underline{x} - \underline{x}'|^2)^{d-1}}. \tag{4.44}$$

Then the field strength tensor F is given by

$$\begin{aligned} F = dA =& (d-1) x_0^{d-3} dx_0 \int d\underline{x}' \frac{a_i(\underline{x}') dx^i}{(x_0^2 + |\underline{x} - \underline{x}'|^2)^{d-1}} \\ & - 2(d-1) x_0^{d-1} dx_0 \int d\underline{x}' \frac{a_i(\underline{x}') dx^i}{(x_0^2 + |\underline{x} - \underline{x}'|^2)^{d}} \\ & - 2(d-1) x_0^{d-3} dx_0 \int d\underline{x}' \frac{a_i(\underline{x}')(x^i - x'^i)(x_k - x'_k) dx^k}{(x_0^2 + |\underline{x} - \underline{x}'|^2)^{d}} \\ & + ... \end{aligned} \tag{4.45}$$

where ... are terms with no dx_0 in.
By applying integration by parts from the product rule for a k-form ω, $d(\omega \wedge \alpha) = (d\omega) \wedge \alpha + (-1)^k \omega \wedge (d\alpha)$.

$$I(A) = \frac{1}{2} \int_{\mathbf{B}_{d+1}} dA \wedge *F \tag{4.46}$$

$$= \frac{1}{2} \int_{\mathbf{S}_d} A \wedge *F + \frac{1}{2} \int_{\mathbf{B}_{d+1}} A \wedge d(*F) \tag{4.47}$$

$$= \frac{1}{2} \lim_{\epsilon \to 0} \int_{T_\epsilon} A \wedge *F, \tag{4.48}$$

again, the second term in (4.47) vanishes due to Maxwell's equations (4.29) with T_ϵ the surface where $x_0 = \epsilon \to 0$. $*F$ is given by

$$\begin{aligned} *F =&(d-1)(-1)^i \int d\underline{x}' \frac{a_i(\underline{x}')d\omega^i}{(x_0^2 + |\underline{x} - \underline{x}'|^2)^{d-1}} \\ &- 2(d-1)(-1)^i x_0^4 \int d\underline{x}' \frac{a_i(\underline{x}')d\omega^i}{(x_0^2 + |\underline{x} - \underline{x}'|^2)^{d}} \\ &- 2(d-1)(-1)^i \int d\underline{x}' \frac{a_k(\underline{x}')(x_i - x_i')(x^k - x'^k)d\omega^i}{(x_0^2 + |\underline{x} - \underline{x}'|^2)^{d}} \\ &+ ..., \end{aligned} \tag{4.49}$$

where $d\omega^i = dx^1 \wedge dx^2 ... \widehat{dx^i} ... \wedge dx^d$ where $\widehat{dx^i}$ means that dx^i is omitted from the wedge product so $dx^j \wedge d\omega^i = (-1)^j \delta^{ij}$. As in the massless scalar case, as $x_0 = \epsilon \to 0$, $A \to A_0$, then in this limit (4.48) gives

$$\begin{aligned} I(A) =&(d-1)(-1)^i \int d\underline{x} d\underline{x}' \frac{a_i(\underline{x}')a_j(\underline{x})dx^j \wedge d\omega^i}{|\underline{x} - \underline{x}'|^{2d-2}} \\ &- 2(d-1)(-1)^i \int d\underline{x}' \frac{a_k(\underline{x}')a_j(\underline{x})(x_i - x_i')(x^k - x'^k)dx^j \wedge d\omega^i}{|\underline{x} - \underline{x}'|^{2d}} \end{aligned} \tag{4.50}$$

$$= (d-1)(-1)^i \int d\underline{x} d\underline{x}' a_i(\underline{x})a_j(\underline{x}') \left(\frac{\delta^{ij}}{|\underline{x} - \underline{x}'|^{2d-2}} - \frac{2(x^i - x'^i)(x^j - x'^j)}{|\underline{x} - \underline{x}'|^{2d}} \right). \tag{4.51}$$

This is of the form of a two-point function for a conserved current. We began with a vector field A_μ with a local $U(1)$ gauge symmetry in the bulk AdS and we obtain the form of a conserved current J_μ two point function with a global $U(1)$ symmetry on the boundary $\partial(AdS)$ ((4.51) is invariant under global rotation of its i,j indices).

4.4.3 Massive scalar in AdS

We may consider the case of a massive scalar field with mass m in AdS_{d+1} space with action

$$I(\phi) = \frac{1}{2} \int d^{d+1}y \sqrt{g} \left(|d\phi|^2 + m^2 \phi^2 \right). \tag{4.52}$$

ϕ obeys the field equation

$$(D_i D^i + m^2)\phi = 0. \tag{4.53}$$

Writing the metric (4.11) in hyperbolic coordinates $d\tilde{s}^2 = dy^2 + (\sinh^2 y) d\Omega^2$ the field equation (4.53) takes the form

$$\left(\frac{-1}{\sinh^d y} \frac{d}{dy} (\sinh^d y) \frac{d}{dy} + \frac{L^2}{\sinh^2 y} + m^2 \right) \phi = 0. \tag{4.54}$$

Where the L^2 term is the angular part of the Laplacian which we can disregard for large y, in this limit $\sinh y \to \frac{1}{2} e^y$, therefore we look for a solution of the form $\phi = e^{\lambda y}$. Then we obtain

$$\lambda(\lambda + d) = m^2. \tag{4.55}$$

We limit m^2 to the region in which the roots are real, and with the larger and smaller roots $\lambda_+ \geq -\frac{d}{2}$ and $\lambda_- \leq -\frac{d}{2}$ picking a linear combination of the two roots then the

solution at the boundary behaves as $e^{\lambda_+ y}$. As in the massless case we would like to find a solution which approaches a constant at the boundary, however $e^{\lambda_+ y}$ clearly diverges at the boundary to remedy this we can pick a function f on $\mathbf{B}_{d+1}$ which approaches zero on the boundary, e.g. $f = e^{-y}$ and then we look for solutions of the form

$$\phi \sim f^{-\lambda_+}\phi_0 \tag{4.56}$$

with ϕ_0 the boundary value. By studying the scaling we see that if $f \to e^{\omega} f$ then $d\tilde{s}^2 \to e^{2\omega} d\tilde{s}^2$ therefore $\phi_0 \to e^{\omega\lambda_+}\phi_0$ from this we deduce that ϕ_0 has mass dimension $-\lambda_+$.

As in the massless case we wish to compute the two point function of the field $\mathcal{O}$ on the boundary, $\mathcal{O}$ will couple to the boundary value of the massive AdS scalar field ϕ_0 as $\int \phi_0 \mathcal{O}$ which must have conformal dimension d, therefore $\mathcal{O}$ must have conformal dimension $(d + \lambda_+)$.

As in the massless case we look for Green's function $G(x_0)$ which obeys the wave equation (4.53) and is a delta function at the point P on the boundary, the solutions must also behave as (4.56) on the boundary located at $x_0 = \infty$. Using the metric as in (4.11). With this metric, and noting the translational invariance, the massive field equation is

$$\left(-x_0^{d+1}\frac{d}{dx_0}x_0^{-d+1}\frac{d}{dx_0} + m^2\right) G(x_0) = 0. \tag{4.57}$$

Picking $G(x_0) = x_0^A$ and using (4.55) $m^2 = \lambda_+(d + \lambda_+)$ then we must choose $A = d + \lambda_+$ to give $G(x_0) = x_0^{d+\lambda_+}$. Which vanishes at $x_0 = 0$ as required, the solution diverges at $x_0 = \infty$ which may be remedied by performing the transformation (4.19) to map the point P to the origin, then

$$G(x) = \frac{x_0^{d+\lambda_+}}{(x_0^2 + |\underline{x}|^2)^{d+\lambda_+}}. \tag{4.58}$$

Using the Green's function $G(x)$ $\phi(x)$ is given by

$$\phi(x) = c\int d\underline{x}' \frac{x_0^{d+\lambda_+}}{(x_0^2 + |\underline{x}|^2)^{d+\lambda_+}}\phi_0(\underline{x}'). \tag{4.59}$$

For $x_0 \to 0$ then $\phi \to x_0^{-\lambda_+}\phi_0$. By applying integration by parts to the action (4.52) we obtain

$$I(\phi) = \frac{1}{2}\int_{\mathbf{S}_d} d^d y x_0^{-(d+1)}(\phi d\phi)\hat{n}_i + \frac{1}{2}\int_{\mathbf{B}_{d+1}} d^{d+1} y x_0^{-(d+1)}\left(\phi dd\phi + m^2\phi^2\right). \tag{4.60}$$

In the limit $x_0 = \epsilon \to 0$ then (4.60)

$$I(\phi) = \frac{1}{2}\lim_{\epsilon\to 0}\int_{T_\epsilon} d\underline{x} x_0^{-d}\phi(\underline{n}.\underline{\nabla})\phi \tag{4.61}$$

with $(n.\nabla)\phi = x_0(\frac{d\phi}{dx_0})$ and in the limit $x_0 = \epsilon \to 0$ we acquire

$$\frac{\partial\phi}{\partial x_0} \approx c(d + \lambda_+)x_0^{d+\lambda_+-1}\int d\underline{x}' \frac{\phi_0(x_i')}{|\underline{x} - \underline{x}'|^{2(d+\lambda_+)}} + O(x_0^{d+\lambda_++1}). \tag{4.62}$$

Noting that $\phi \to x_0^{-\lambda_+}\phi_0(x)$ as $x_0 \to 0$, thus evaluating the action in this limit (4.61) we get

$$I(\phi) = \frac{c(d+\lambda_+)}{2}\int d\underline{x}d\underline{x}' \frac{x_0^{-d}x_0^{-\lambda_+}\phi_0(\underline{x})x_0^{d+\lambda_+-1}\phi_0(\underline{x}')}{|\underline{x}-\underline{x}'|^{2(d+\lambda_+)}} \tag{4.63}$$

$$= \frac{c(d+\lambda_+)}{2}\int d\underline{x}d\underline{x}' \frac{\phi_0(\underline{x})\phi_0(\underline{x}')}{|\underline{x}-\underline{x}'|^{2(d+\lambda_+)}}. \tag{4.64}$$

This is the form of a two-point function of a conformal field $\mathcal{O}$ of conformal dimension $\Delta = d + \lambda_+$ as ϕ_0 has mass dimension $-\lambda_+$. Thus the dimension of a conformal field on the boundary that is the holographic dual to a field of mass m in AdS_{d+1} $\Delta = d + \lambda_+$ is is related to the mass as the largest root of $m^2 = \Delta(\Delta - d)$. Thus dimensions of boundary correlation functions are dependent on the masses of the particles in the supergravity theory.

Chapter 5

Entanglement Entropy's from the AdS/CFT Correspondence

5.1 Entanglement Entropy & Holography

We would like to calculate entanglement entropy's in CFT's, to calculate the entanglement entropy directly from the CFT side using standard field theory methods, i.e. constructing path integrals to then obtain density matrices and taking traces, is extremely complex for arbitrary d and analytical results are hard to find. It has been proposed by Ryu and Takayanagi [31, 30] that the AdS/CFT correspondence may be used to calculate CFT entanglement entropy's. Suppose that we have CFT_{d+1} theory, the AdS/CFT correspondence says that there is a dual to AdS_{d+2} space and the CFT_{d+1} lives on the AdS_{d+2} $d+1$ dimensional boundary $\partial(AdS)$. If a region of the boundary is divided into two subsystems A and B, where B covers the entire boundary region $B \cap A$, the entanglement entropy of subsystem A with subsystem B is given by the area of the minimal surface γ_A which extends from the region A on the boundary $\partial(AdS)$ into the bulk AdS and then the entanglement entropy is given by a simple area law which was postulated from the form of (4.2) [29]

$$S_A = \frac{Area(\gamma_A)}{4G_N^{(d+2)}}, \tag{5.1}$$

where $G_N^{(d+2)}$ is Newton's constant in $d+2$ dimensions.

In this section entanglement entropy's in static, fixed time geometries will be calculated for varying geometries from the point of view of the $AdS_{d+2}/\text{CFT}_{d+1}$ correspondence. In these cases the manifold γ_A is a d dimensional, fixed t, minimal area surface extending from the region A on the d dimensional AdS boundary. To obtain a meaningful field theory result we must be able to relate the dimensional constants of the AdS theory to those of the CFT, most importantly, in AdS_3, the relation between the CFT central charge c to the AdS radius R and Newtons Constant G_N is given by [9, 32, 29]

$$c = \frac{3}{2G_N^{(3)}\sqrt{|\Lambda|}}. \tag{5.2}$$

Applying the relation between R and the cosmological constant $\Lambda = -\frac{(d-1)(d-2)}{2R^2}$, for AdS_3/CFT_2 we obtain

$$c = \frac{3R}{2G_N^{(3)}}. \tag{5.3}$$

5.2 Entanglement Entropy Calculations for CFT$_{1+1}$/AdS_{2+1}

5.2.1 Entanglement Entropy of a line in CFT$_{1+1}$

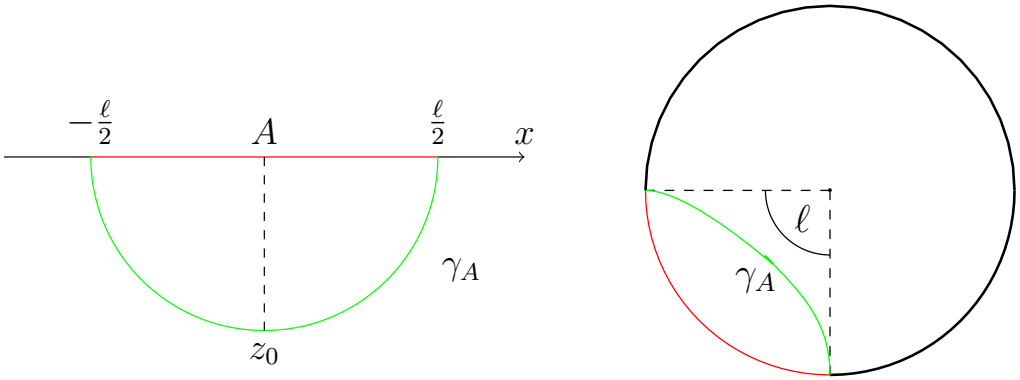

(a) (b)

Figure 5.1: (a) Illustration of γ_A in AdS_{2+1} with boundary $\mathbb{R}^{1,1}$. (b) Illustration of γ_A in AdS_{2+1} with boundary $\mathbb{R}^1 \times \mathbb{S}^1$.

The entanglement entropy for a CFT$_{1+1}$ can be calculated. The entangled region A is taken to be a line of length ℓ lying on the infinite line $\mathbb{R}^{1,1}$ at a fixed time $t = t_0$. The calculation is best performed in Poincaré coordinates (5.4) which gives the half-space parametrization of AdS with a boundary located at $z \to 0$ which is conformally equivalent to Minkowski space

$$ds^2 = R^2 \frac{-dt^2 + dz^2 + \sum_{i=1}^{d-1} dx_i^2}{z^2}. \tag{5.4}$$

The area of the minimal area surface γ_A which extends into the bulk of AdS reduces to finding the geodesic length in AdS_{2+1} [31, 2]. The length of the geodesic is given by minimising the action

$$Length(\gamma_A) = 2R \int_0^{z_0} \frac{1}{z} \sqrt{1 + \left(\frac{dx}{dz}\right)^2}\, dz. \tag{5.5}$$

Applying the Euler-Lagrange equations we obtain the equation of motion

$$x^2 + z^2 = z_0^2. \tag{5.6}$$

Applying the boundary condition $x(z_0) = 0$, $x(0) = \pm\frac{\ell}{2}$ the geodesic is parametrized by a semi-circle with radius $z_0 = \frac{\ell}{2}$ and is symmetric about the midpoint z_0, as shown in Fig.(5.1a).

$$\begin{aligned} Length(\gamma_A) &= \ell R \int_\epsilon^{\frac{\ell}{2}} \frac{1}{z} \sqrt{\left(\frac{\ell^2}{4} - z^2\right)^{-1}}\, dz \\ &= 2R \int_{\arcsin\left(\frac{2\epsilon}{\ell}\right)}^{\frac{\pi}{2}} \frac{d\theta}{\sin\theta} \\ &= 2R \log\left(\frac{\ell}{\epsilon}\right), \end{aligned} \tag{5.7}$$

where $\epsilon \to 0$ is a UV cutoff which must be imposed due to the logarithmic divergence at $z = 0$. It is satisfying that this divergence is produced, as it reproduces the type of UV regularization treatment required to deal with the infinite UV degrees of freedom found in QFT's. Applying (5.1) and (5.3) the entanglement entropy is given by

$$S_A = \frac{Length(\gamma_A)}{4G_N^{(3)}} = \frac{c}{3}\log\left(\frac{\ell}{\epsilon}\right) \tag{5.8}$$

where $G_N^{(3)}$ is Newton's gravitational constant in 3 dimensions. This matches the results found in [21, 11].

5.2.2 Entanglement Entropy on a circle in CFT$_{1+1}$

The calculation can be performed for the case where the spatial dimension x is compactfied to give a $\mathbb{R}^1 \times \mathbf{S}^1$ boundary geometry. The region A is now described by the angle ℓ as shown in Fig.(5.1b). The calculation is best performed in the global coordinates of AdS

$$ds^2 = R^2\left(-(1+r^2)dt^2 + \frac{dr^2}{(1+r^2)} + r^2 d\Omega_{d-1}^2\right), \tag{5.9}$$

with $d\Omega_{d-1}^2$ the metric of a $d-1$-sphere $\mathbf{S}^{d-1}$. Which gives, for AdS_3 on $\mathbf{S}^1$, the geodesic length

$$Length(\gamma_A) = 2R\int_{r_0}^{\infty}\sqrt{\frac{1}{1+r^2} + r^2\left(\frac{d\phi}{dr}\right)^2}\,dr, \tag{5.10}$$

where r_0 is the minimum value obtained by the radial coordinate. Applying the Euler-Lagrange equations to (5.10)

$$\left(\frac{d\phi}{dr}\right)^2 = \frac{r_0^2}{r^2(1+r^2)(r^2-r_0^2)}. \tag{5.11}$$

Applying the boundary conditions $r(0) = r_0$, $r(\frac{\ell}{2}) = \infty$ and performing the integral we find the equation of motion

$$\phi = -\frac{1}{2}\arcsin\left(\frac{\frac{2}{r^2} - \frac{1}{r_0^2} + 1}{\frac{1}{r_0^2}}\right) + \frac{\pi}{4} \tag{5.12}$$

applying the boundary conditions we find the relation $r_0^2 = \frac{1}{\tan^2(\frac{\ell}{2})}$. Performing the integral and imposing the same UV cutoff as in (5.8) at $r = \infty \to \frac{1}{\epsilon}$, by applying (5.1) and (5.3) the entanglement entropy is given by

$$S_A = \frac{Length(\gamma_A)}{4G_N^{(3)}} = \frac{c}{3}\log\left(\frac{2\sin\left(\frac{\ell}{2}\right)}{\epsilon}\right) \tag{5.13}$$

For small ℓ (5.13) reproduces the result from (5.8) as expected, as in the neighbourhood of $\ell = 0$ on $\mathbf{S}^1$ the entanglement entropy perceives a $\mathbb{R}^1$ geometry.

5.3 Strong Subadditivity

It has been proved entanglement entropy must manifest the property of strong subadditivity [20], given by the following inequalities:

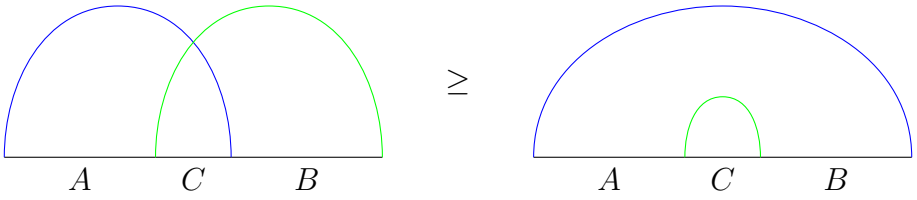

$$S_{A+C} + S_{B+C} \geq S_{A+B+C} + S_C \tag{5.14}$$

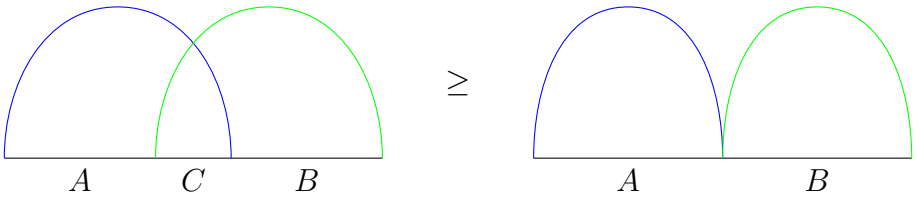

$$S_{A+C} + S_{B+C} \geq S_A + S_B \tag{5.15}$$

It is possible, for the case of $\mathrm{CFT}_{1+1}/AdS_{2+1}$ in global coordinates to show that (5.13) does indeed exhibit the property of Strong Subadditivity. (5.14) may be proved as follows. We take the total length of the system $\ell_T = \ell_{AC} + \ell_{BC} - \ell_C = \ell_A + \ell_B \geq 0$. The entanglement entropy is bounded between its minimal and maximal values $0 \leq S \leq \log\left(\frac{2}{\epsilon}\right)$, thus $0 \leq \ell_T \leq \pi$. To show (5.14) we consider the UV cutoff independent part of (5.13), so subtracting the constant UV divergent term $\log\left[\frac{2}{\epsilon}\right]$ and assuming (5.14) to be true we obtain

$$\log\left[\sin\left(\frac{\ell_{AC}}{2}\right)\right] + \log\left[\sin\left(\frac{\ell_{BC}}{2}\right)\right] \geq \log\left[\sin\left(\frac{\ell_{AB}}{2}\right)\right] + \log\left[\sin\left(\frac{\ell_C}{2}\right)\right], \tag{5.16}$$

simplifying

$$\cos\left(\frac{\ell_{AC} - \ell_{BC}}{2}\right) \geq \cos\left(\frac{2\ell_T - \ell_{AC} - \ell_{BC}}{2}\right), \tag{5.17}$$

thus (5.14) is proved as $\ell_{AC} \leq \ell_T \leq \pi$. (5.15) may also be proved as follows, assuming the relation is true we have

$$\log\left[\sin\left(\frac{\ell_{AC}}{2}\right)\right] + \log\left[\sin\left(\frac{\ell_{BC}}{2}\right)\right] \geq \log\left[\sin\left(\frac{\ell_A}{2}\right)\right] + \log\left[\sin\left(\frac{\ell_B}{2}\right)\right] \tag{5.18}$$

using the relations $\ell_A = \ell_{AC} - \alpha\ell_C$ and $\ell_B = \ell_{BC} - \beta\ell_C$ with $\alpha + \beta = 1$

$$\sin\left(\frac{\ell_{AC}}{2}\right)\sin\left(\frac{\ell_{BC}}{2}\right) \geq \sin\left(\frac{\ell_{AC} - \alpha\ell_C}{2}\right)\sin\left(\frac{\ell_{AC} - \beta\ell_C}{2}\right) \tag{5.19}$$

therefore (5.15) is proved as all the arguments appearing in the sine's are bounded between zero and $\frac{\pi}{2}$ therefore both sides are bound between zero and unity therefore the right hand side of (5.19) will always be greater than or equal to the left hand side.

5.4 Entanglement entropy of an infinite strip in $AdS_{d+2}/\mathbf{CFT}_{d+1}$

The entanglement entropy of an infinite strip for a CFT_{d+1} on $\mathbb{R}^{1,d}$ at a fixed time slice can be calculated [31]. The entangled region A is taken to be a strip of infinite length $L \to \infty$ in $d-1$ spatial directions and of length ℓ in the remaining spatial direction. We must find the minimal surface γ_A which extends from the boundary region A into the AdS bulk. Using the metric (5.4)

$$Area(\gamma_A) = 2\int_0^L dx_2 ... \int_0^L dx_d \int_0^{z_0} \sqrt{g|_{induced}}dz \tag{5.20}$$

$$= 2R^d L^{d-1} \int_0^{z_0} \frac{1}{z^d}\sqrt{1+\left(\frac{dx_1}{dz}\right)^2}dz, \tag{5.21}$$

where z_0 is a constant of the motion and is physically a turning point located at the maximum value obtained by the radial coordinate z. The surface is therefore symmetric about this point z_0. Minimising (5.21) we obtain the equation of motion

$$\left(\frac{dx_1}{dz}\right) = \sqrt{\frac{z^{2d}}{z_0^{2d}-z^{2d}}}. \tag{5.22}$$

Integrating and performing the substitution $p = \frac{z}{z_0}$

$$\int_0^{\frac{\ell}{2}} dx_1 = z_0 \int_0^1 \frac{p^d}{\sqrt{1-p^{2d}}}dp. \tag{5.23}$$

Employing the standard definite integral

$$\int_0^1 t^{\alpha-1}(1-t^\lambda)^{\beta-1}dt = \frac{B(\frac{\alpha}{\lambda},\beta)}{\lambda} = \frac{\Gamma(\frac{\alpha}{\lambda})\Gamma(\beta)}{\lambda\Gamma(\frac{\alpha}{\lambda}+\beta)} \tag{5.24}$$

gives the relation between ℓ and z_0

$$\frac{\ell}{2} = z_0 \frac{\Gamma(\frac{d+1}{2d})\sqrt{\pi}}{\Gamma(\frac{1}{2d})}. \tag{5.25}$$

Combining (5.22) and (5.21) and performing the substitution $p = \frac{z}{z_0}$

$$Area(\gamma_A) = 2R^d L^{d-1} z_0^{1-d} \int_0^1 \frac{1}{p^d}\frac{1}{\sqrt{1-p^{2d}}} \tag{5.26}$$

the $\frac{1}{p^d}$ part of the integral is UV divergent, we may rearrange to deal with the divergence

$$Area(\gamma_A) = 2R^d L^{d-1} z_0^{1-d}\left[\int_0^1 \frac{dp}{p^d} + \int_0^1 \frac{dp}{p^d}\left(\frac{1}{\sqrt{1-p^{2d}}}-1\right)\right]. \tag{5.27}$$

The first term of this integral is UV divergent so we must regulate this term with a UV cutoff near $z=0$ at this point $z=\epsilon \to 0$ and now the second term is finite, employing (5.24) we obtain

$$Area(\gamma_A) = 2R^d L^{d-1} z_0^{1-d}\left[\frac{1}{d-1}\left(\frac{z_0}{\epsilon}\right)^{d-1} - \frac{\sqrt{\pi}\Gamma(\frac{1-d}{2d})}{2d\Gamma(\frac{1}{2d})}\right]. \tag{5.28}$$

Combining (5.28), (5.25) and (5.1) we obtain the result for the entanglement entropy

$$S_A = \frac{R^d}{(d-1)4G_N^{(d+2)}} \left[2\left(\frac{L}{\epsilon}\right)^{d-1} - 2^d\sqrt{\pi}^d \left(\frac{\Gamma(\frac{d+1}{2d})}{\Gamma(\frac{1}{2d})}\right)^d \left(\frac{L}{\ell}\right)^{d-1} \right]. \tag{5.29}$$

The result dimensionally matches the expected field theory result of being proportional to the area of the boundary $\partial(AdS)$. Due to the introduction of a new length scale L we find both a UV divergent term as well as a finite term in which we can directly compare entanglement entropy between systems.

5.5 Spherical strip in AdS_4 and phase transitions and confinement

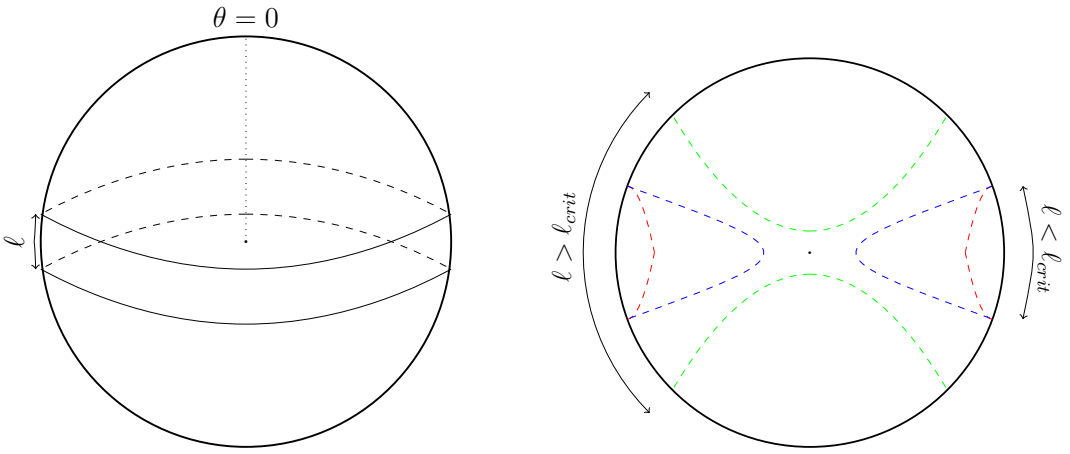

Figure 5.2: (b) Geometrical setup of spherical strip in AdS_4. (b) Illustration of surfaces in AdS_4 projected in the $\theta = 0$ plane.

The prescription (5.1) is repeated for the case of a CFT_3 on a spatially compact $\mathbb{R}^1 \times \mathbf{S}^2$ boundary of AdS_4 and the entangled region A is taken to be a spherical strip of width ℓ, symmetrical about the $\theta = \frac{\pi}{2}$ plane, as shown in 5.2. In this geometry we expect to find a phase transition between minimal surface γ_A solutions for a critical value of the strip width $\ell = \ell_{crit}$ as illustrated in Fig.(5.2a). The AdS_4 metric in global coordinates, working in units where the AdS radius $R = 1$ which may be reintroduced by dimensional analysis, is given by

$$ds^2 = -\left(1 + r^2\right) dt^2 + \frac{1}{(1+r^2)} dr^2 + r^2(d\theta^2 + \sin^2\theta d\phi^2). \tag{5.30}$$

We consider a fixed time slice and by considering the spherical symmetry $0 \leq \phi \leq 2\pi$, and the symmetry of the surfaces about the $\theta = \frac{\pi}{2}$ plane and with respect to the midpoint where the radial coordinate reaches a minimum value $r = r_0$ then $r_0 < r < \delta$, with $\delta \to \infty$ a UV cutoff imposed near the boundary. The area of the surface γ_A may be obtained by taking twice the surface in only the upper hemisphere

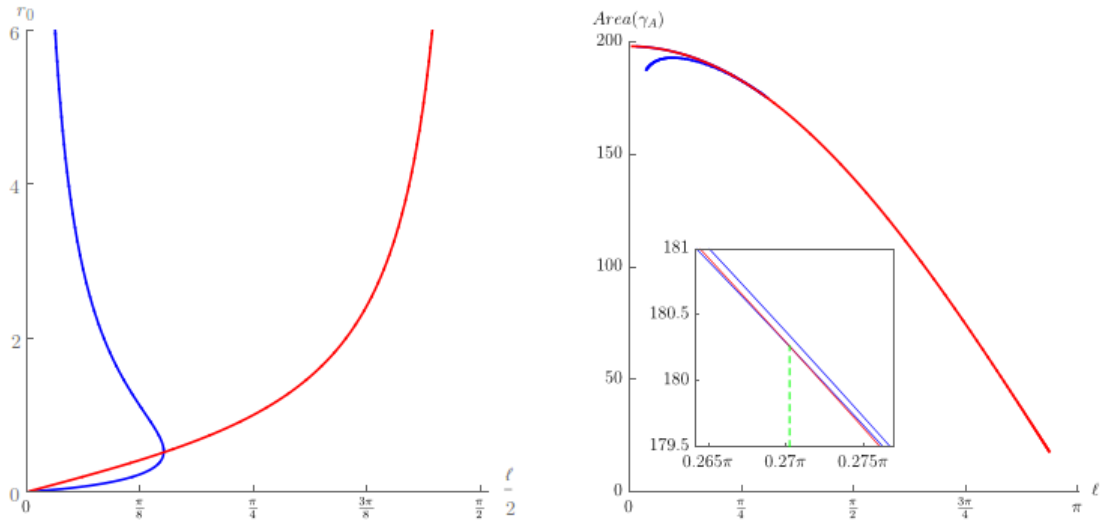

(a) (b)

Figure 5.3: (a) Plot of r_0 against $\frac{\ell}{2}$. (a) Plot of Area(γ_A against ℓ and on the inset the same plot zoomed in close to ℓ_{crit} indicated by the dashed line.

with values of θ between $\frac{\pi-\ell}{2} \leq \theta \leq \frac{\pi}{2}$. The area of the surface is then given by

$$Area(\gamma_A) = 2\int_0^{2\pi}\int_{r_0}^{\delta}\sqrt{g}d\phi dr = 4\pi\int_{r_0}^{\delta} r\sin^2\theta\sqrt{r^2\left(\frac{d\theta}{dr}\right)^2 + \frac{1}{1+r^2}}dr \tag{5.31}$$

where g is the determinant of the metric induced on the surface. Minimizing the action (5.31) we obtain the equation of motion

$$\frac{d}{dr}\left(\frac{r^3\theta'\sin\theta}{\sqrt{\frac{1}{1+r^2}+r^2\theta'^2}}\right) = \sqrt{r^2\cos^2\theta\left(\frac{1}{1+r^2}+r^2\theta'^2\right)} \tag{5.32}$$

where primes denote $\frac{d}{dr}$.

We expect to find 3 classes of solutions, as illustrated in Fig.(5.2b). Two connected solutions which cross $\theta = \frac{\pi}{2}$ where the piece of the surface coming from $\theta = \frac{\pi-\ell}{2}$ joins with the piece coming from $\theta = \frac{\pi+\ell}{2}$ at $\theta = \frac{\pi}{2}$, one of these type of solutions stays close to the boundary, the other type of solution extends deep into the AdS_4 bulk and obtains a minimum radial value r_0 very close to $r_0 = 0$. The latter of these solutions will clearly be always unfavoured as these types of solutions as they do not minimize (5.31). We also find a disconnected solution appearing as two caps in either hemisphere where the two pieces of the minimal surface in each hemisphere do not join and they cross $\theta = \frac{\pi}{2}$. A phase transition between connected and disconnected solutions is seen for a critical value of the width of the entangling region ℓ_{crit}.

Analytic solutions to (5.32) are not easily obtained, we may solve the problem numerically, for the two classes of solution we must integrate with the boundary conditions

$$\begin{cases} \theta(r_0) = \frac{\pi}{2}, & \theta'(r_0) = -\infty & \text{Connected} \\ \theta(r_0) = 0, & \theta'(r_0) = \infty & \text{Disconnected.} \end{cases}$$

We find that the connected solution is bounded between values of $0 < \ell \lesssim 0.3\pi$ as shown in Fig.(5.3a) and that for each value of ℓ in that range there are two possible values of r_0 corresponding to the two types of connected solutions pictured in Fig.(5.2b). From Fig.(5.3b) the value of ℓ_{crit} is numerically obtained to be $\ell_{crit} \approx 0.27\pi$. For values of $\ell > \ell_{crit}$ the disconnected solution is favoured as shown in Fig.(5.3b), for this solution as ℓ increases from the point ℓ_{crit} the entanglement entropy decreases as the area of the CFT region A on the boundary becomes ever larger than it's complement region B, the rest of the system. Then the entanglement entropy approaches 0 as ℓ approaches $\ell = \pi$. The transition between solution types is characteristic of a first order phase transition.

As a demonstration, an analogous phase transition is seen for AdS_3/CFT_2 with $\mathbb{R}^1 \times \mathbf{S}^1$ boundary, an analytical result for ℓ_{crit} may be obtained form the result (5.13). In this case a disconnected solution is favoured for $\ell < \ell_{crit}$ and a connected solution for $\ell > \ell_{crit}$, then

$$S_A^{dis} = 2\log\left(\frac{2\sin\left(\frac{\ell}{2}\right)}{\epsilon}\right), \tag{5.33}$$

$$S_A^{con} = 2\log\left(\frac{2\sin\left(\frac{\pi-\ell}{2}\right)}{\epsilon}\right) \tag{5.34}$$

equating (5.33) and (5.34) we obtain $\ell_{crit} = \frac{\pi}{2}$.

5.5.1 Entanglement Entropy as an indication of a confinement/deconfinement phase transition

An interpretation of this phase transition between minimal surfaces in terms of the boundary CFT is that of a confinement/deconfinement phase transition [35, 24]. In [24] a similar type of phase transition was demonstrated for the gravitational dual of Large-N Yang-Mills gauge theory and it was proposed that the Entanglement Entropy could be used as a probe of confinement based upon the scaling of the entanglement entropy.

In [24] the considered QFT is a confining gauge theory with a mass gap, consequently the gravitational dual of such a theory has an IR cutoff far from the boundary at a fixed value in the radial coordinate. The gravitational dual to the field theory considered in the spherical strip case is empty AdS_4, therefore the field theory it describes is a CFT and thus is expected to have no mass gap and therefore exhibit no confinement, however when placing the theory on a compact, closed manifold with therefore finite volume, momenta in the boundary theory become necessarily quantised, thus inducing a mass gap. Finite volume effects can induce confinement in the boundary CFT.

As seen in (5.29) the entanglement entropy of infinite strip for a CFT_{d+1} on the non-compact $\mathbb{R}^{1,d}$ boundary of AdS_{d+2} is non-periodic and the UV divergent independent part behaves as $-(\frac{L}{\ell})^d$, therefore only a single, connected, type of solution is seen thus there is no confining phase. This further implies that finite volume effects are inducing confinement. The reason is as follow, when on non-compact, infinite space, e.g. $\mathbb{R}^d$ we have no conditions at the boundary, only that fields should die off at spatial infinity, thus there are no constraints on global states carrying a gauge charge. When the field theory is placed on a compact space with a finite volume, in this case $\mathbf{S}^2$, then by Gauss' Law there is now conditions at the

boundary and therefore globally we must have only bound, gauge invariant states of the form $\overline{\psi}\psi$.

In terms of entanglement entropy and the transition between minimal surface types, the interpretation is that for $\ell < \ell_{crit}$ the entanglement entropy is probing the confined degrees of freedom of the gauge invariant states. For $\ell > \ell_{crit}$ the entanglement entropy no longer has access to the degrees of freedom inside the gauge invariant bound states and the entanglement entropy probes the exterior degrees of freedom of the bound states.

Chapter 6

Thermal CFT's and AdS black holes

6.1 Entanglement Entropy in Thermal CFT's

The entanglement entropy for a region A of length of ℓ CFT_2 on $\mathbb{R}^{1,1}$ at finite temperature β_{CFT}^{-1} can be calculated using the AdS/CFT correspondence. The holographic gravity dual is given by the non-rotating Euclidean BTZ Black Hole (6.1) [4, 13] which may be obtained by performing a Wick rotation $t \to i\tau$ on the Minkowski signature BTZ Black Hole metric and imposing periodicity $\tau \sim \tau + \frac{2\pi R}{r_+}$ to ensure that conical singularities do not arise as $r \to 0$ to obtain $\mathbf{S}^1 \times \mathbb{R}^1$ boundary geometry. The BTZ black hole temperature is given by the Hawking temperature $T_{BTZ} = \beta_{BTZ}^{-1} = \frac{2\pi R}{r_+}$. The Euclidean BTZ Black hole is given by

$$ds^2 = \frac{\left(r^2 - r_+^2\right)}{R^2} d\tau^2 + \frac{R^2}{r^2 - r_+^2} dr^2 + r^2 d\phi^2. \tag{6.1}$$

The holographic dictionary provides us with a method to obtain the dual CFT_2 stress-energy tensor. The holographic dictionary tells us that for a CFT with a dual that is asymptotically AdS the CFT stress tensor on the boundary may be obtained by first casting the metric into Fefferman-Graham form [15, 16, 3]

$$ds^2 = \frac{R^2}{\rho^2} \left(d\rho^2 + g_{ij}(x, \rho) dx^i dx^j\right) \tag{6.2}$$

where $g_{ij} = g_{ij}^{(0)} + g_{ij}^{(2)} \rho^2 + ... + g_{ij}^{(d)} \rho^d + ...$, where d is the CFT dimension. Then the CFT stress energy tensor may be read off from the normalizable modes of the metric (6.2), the interpretation of this is that the non-normalizable modes act as sources at infinity for the boundary fields. The CFT stress energy tensor is [14]

$$\langle T_{ij} \rangle_{CFT} = \frac{dR^{d-1}}{16\pi G_N^{(d+1)}} g_{ij}^{(d)} + X_{ij}[g^n] \tag{6.3}$$

where $X_{ij}[g^n]$ is a function of the FG metric for $n < d$ and reflects the conformal anomaly in even d systems. For $d = 2$ [14]

$$\langle T_{ij} \rangle_{CFT} = \frac{2R}{16\pi G_N^{(3)}} \left(g_{ij}^{(2)} - g_{ij}^{(0)} \operatorname{Tr}\left(g_{ij}^{(2)}\right)\right). \tag{6.4}$$

The metric (6.1) is in AdS-Schwarzchild form and must first be cast in Fefferman-Graham form (6.2), noting that we require the radial coefficient $= \frac{1}{\rho^2}$ we apply the coordinate transformation $\frac{d\rho}{\rho} = \frac{dr}{\sqrt{r^2-r_+^2}}$ [33, 5] giving

$$\int \frac{d\rho}{\rho} = \int \frac{dr}{\sqrt{r^2 - r_+^2}} \tag{6.5}$$

$$\rho = A(r + \sqrt{r^2 - r_+^2}) \tag{6.6}$$

picking $A = \frac{2}{r_+^2}$ so that for $r \to \infty$, $\rho \to \frac{1}{r}$, then

$$r = \frac{1}{\rho} + \frac{r_+^2 \rho}{4}, \tag{6.7}$$

therefore the boundary with this choice of Fefferman-Graham coordinates is located at $\rho = 0$. Inserting into (6.1) and using the relationship $\frac{r_+^2}{R^2} = m$, we obtain the Euclidean BTZ black hole metric in Fefferman-Graham form

$$ds^2 = \frac{R^2}{\rho^2}\left(d\rho^2 + \left(\frac{R^2 m^2 \rho^4}{16} + \frac{1}{R^2} - \frac{m\rho^2}{2}\right)d\tau^2 + \left(\frac{R^2 m^2 \rho^4}{16} + \frac{1}{R^2} + \frac{m\rho^2}{2}\right)dx^2\right). \tag{6.8}$$

Asymptotically $\rho \to 0$ (6.8) has the form of flat Euclidean space $ds^2 \to d\tau^2 + dx^2$. Applying (6.4) to the metric (6.8), reversing the Wick rotation $\tau \to it$ and noting that $\mathrm{Tr}\,(g_{ij}^{(2)}) = 0$, we obtain the boundary CFT_2 stress-energy tensor

$$\langle T_{ij} \rangle_{CFT} = \frac{R}{16\pi G_N^{(3)}} \begin{pmatrix} -m & 0 \\ 0 & m \end{pmatrix}. \tag{6.9}$$

Giving the pressure and energy density

$$\epsilon = -\langle T_{tt} \rangle_{CFT} = \frac{Rm}{16\pi G_N^{(3)}}, \tag{6.10}$$

$$p = \langle T_{xx} \rangle_{CFT} = \frac{Rm}{16\pi G_N^{(3)}}. \tag{6.11}$$

We see that the stress-energy tensor is traceless $\langle T_i^i \rangle_{CFT} = 0$ which is characteristic of a conformally invariant system which may be shown as thus. Conserved currents in conformal field theory are given by $J_\mu = T_{\mu\nu}x^\nu$ where $\partial^\mu J_\mu = 0$ [37]. These J_μ's are the conserved currents associated with the conformal scaling symmetries $x^\mu \to \sigma x^\mu$ where σ denotes a scale transformation. Because the stress-energy tensor is conserved by definition $\partial^\mu T_{\mu\nu} = 0$, then

$$\partial^\mu J_\mu = \partial^\mu T_{\mu\nu} x^\nu \tag{6.12}$$

$$= (\partial^\mu T_{\mu\nu})x^\nu + T_{\mu\nu}(\partial^\mu x^\nu) \tag{6.13}$$

$$= T_{\mu\nu}\delta^{\mu\nu} \tag{6.14}$$

$$= T_\mu^\mu \equiv 0. \tag{6.15}$$

We now wish to calculate the entanglement entropy for a CFT_2 at thermal equilibrium, following the Ryu-Takayanagi prescription for the entanglement entropy

(5.1) [31] we must find the area of the minimal surface γ_A which extends from the region A of length ℓ on the boundary CFT_2 into the bulk AdS_3 geometry. As in the CFT_2 at zero temperature, the minimal surface is given by finding the geodesic length

$$Length\,(\gamma_A) = 2\int_{r_0}^{\delta} \sqrt{\frac{R^2}{r^2 - r_+^2} + r^2\left(\frac{d\phi}{dr}\right)^2}\, dr. \tag{6.16}$$

Where a UV cutoff $\delta \to \infty$ must be introduced to regulate the theory and r_0 is the minimum value obtained by the radial coordinate r about which point the geodesics are symmetric. Minimising the action and applying the substitution $y = \frac{1}{r^2} - \frac{1}{2}(\frac{1}{r_+^2} + \frac{1}{r_0^2})$ the equation of motion is obtained

$$\phi = -\frac{R}{2r_+}\int \frac{dy}{\sqrt{y^2 - c^2}} = \frac{R}{2r_+}\arcsin\left(\frac{y}{c}\right) + B \tag{6.17}$$

with $c^2 = \frac{1}{4}(\frac{1}{r_+^2} + \frac{1}{r_0^2})^2 - \frac{1}{r_0^2 r_+^2}$. The constant of integration B is fixed by applying the boundary condition $\phi(r_0) = 0$ giving

$$\phi(r) = -\frac{R}{2ir_+}\arcsin\left(\frac{2r_+^2 r_0^2 - r^2(r_0^2 + r_+^2)}{r^2 r_0^2 - r^2 r_+^2}\right) - \frac{R\pi}{4ir_+}. \tag{6.18}$$

Applying the remaining boundary condition $\phi(\infty) = \frac{\ell}{2}$ the relation between ℓ and r_0 is obtained

$$r_0 = r_+ \coth^2\left(\frac{r_+\ell}{2R}\right). \tag{6.19}$$

Combining (6.19) and (6.16) with the substitutions $z = r^2 - \frac{1}{2}(r_+^2 + r_0^2)$, $k^2 = \frac{1}{4}(r_+^2 + r_0^2)^2 - r_+^2 r_0^2$ and expanding the result for $\delta = \infty$

$$Length\,(\gamma_A) = R\int_{\frac{1}{2}(r_0^2 - r_+^2)}^{\delta} \frac{dz}{\sqrt{z^2 - k^2}} \tag{6.20}$$

$$= 2R\log\left[\frac{2\delta}{r_+}\sinh\left(\frac{\ell r_+}{2R}\right)\right]. \tag{6.21}$$

According to the holographic dictionary the CFT inverse temperature with respect to the BTZ Black Hole inverse temperature is $\beta_{BTZ} = \beta_{CFT}^{-1}$ and the AdS_3 UV cutoff δ is to be interpreted as $\delta = \frac{\beta_{CFT} r_+}{2\pi\epsilon}$ with respect to the field theory UV cutoff $\epsilon \to 0$ therefore, using (5.1)

$$S_A(\ell, \beta_{CFT}) = \frac{c}{3}\log\left[\frac{\beta_{CFT}}{\pi\epsilon}\sinh\left(\frac{\pi\ell}{\beta_{CFT}}\right)\right]. \tag{6.22}$$

For the case of empty AdS_3 $\beta_{CFT} = 0$ and we recover the expected CFT vacuum result $S_A(\ell) = \frac{c}{3} log \frac{\ell}{\epsilon}$. For large values of the entangled region A where $\frac{\ell}{\beta_{CFT}} \gg 1$ the entanglement entropy becomes $S_A(\ell, \beta_{CFT}) \approx \frac{c}{3}\log\left[\frac{\beta_{CFT}}{2\pi\epsilon} e^{\frac{\pi\ell}{\beta_{CFT}}}\right] = \frac{c}{3}\left(\log\left(\frac{\beta_{CFT}}{2\pi\epsilon}\right) + \frac{\pi\ell}{\beta_{CFT}}\right)$. In this regime the UV independent part of the entanglement entropy behaves like an extensive quantity in ℓ.

Chapter 7

Holographic Quantum Quenches

As found in the last section the holographic dual of a CFT_2 at finite temperature is the static BTZ black hole, which gives the entanglement entropy (6.22).

We wish to now to study dynamical, time evolving systems, specifically studying a CFT system undergoing a quantum quench. The entanglement entropy can be used to measure the propagation of entanglement as the system evolves through time.

In general a quantum quench is where we take a quantum system which begins in a pure state $|\Psi_0\rangle$ and suddenly switch on a parameter in the Hamiltonian to push the system away from equilibrium and then we may study the evolution of the system as it relaxes and returns to a new equilibrium like state $|\Psi(t)\rangle$ at a later time t.

In [10] analytical results were obtained for a critical quantum quench performed on a CFT_{1+1}. Analytic results in higher dimensions are harder to obtain. We may study the effect of a quantum quench on a CFT from the viewpoint of the AdS/CFT correspondence. The gravitational dual to such a process is described by Vaidya solutions [1]. Vaidya solutions describe the collapse of null dust resulting in the formation of a black hole. Generally Vaidya solutions are Schwarzschild-like solutions written in ingoing Eddington-Finkelstein coordinates, where the black hole mass is no longer fixed but becomes a dynamical variable.

The Vaidya geometry describes the dynamical collapse of null dust along an ingoing lightcone coordinate v which results in the formation of a black hole. Examining the Penrose diagram 7.1 we see that geodesics coming from $r = \infty$ at finite t perceive a pure BTZ geometry and as the geodesics move to smaller values of r they can pass behind the apparent horizon. As geodesics move towards $v \to -\infty$, $r \to 0$ they percive a pure AdS geometry.

The metric for the static Schwarzschild-AdS_{d+1} black hole of mass m, setting the AdS curvature radius $R = 1$, is given by

$$ds^2 = -(r^2 - \frac{m}{r^{d-2}})dt^2 + \frac{1}{r^2 - \frac{m}{r^{d-2}}}dr^2 + r^2 \sum_{i=1}^{d-1} dx_i^2, \tag{7.1}$$

which may be written in Eddington-Finkelstein coordinates with the coordinate change

$$v = t + f(r), \quad \frac{df(r)}{dr} = \frac{r^{d-2}}{r^d - m}. \tag{7.2}$$

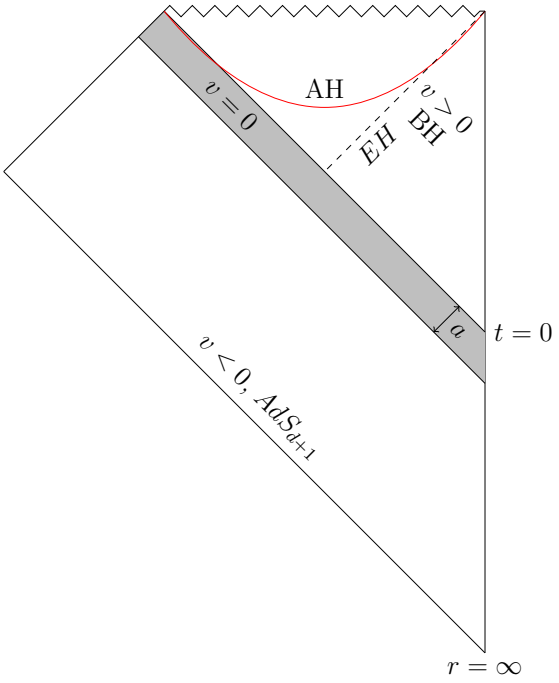

Figure 7.1: AdS_{d+1}-Vaidya Penrose diagram [25, 7] BH denotes the black hole region, AH denotes the location of the apparent horizon, EH denotes the location of the black hole event horizon.

By then allowing m to depend on the coordinate v, $m \to m(v)$, we obtain the AdS_{d+1}-Vaidya metric with boundary $\mathbb{R}^{1,d}$ which are solutions to Einsteins equations

$$ds^2 = -\left(r^2 - \frac{m\,(v)}{r^{d-2}}\right) dv^2 + 2dvdr + r^2 \sum_{i=1}^{d-1} {dx_i}^2. \tag{7.3}$$

Close to the boundary $r \to \infty$, $f'(r) \simeq \frac{1}{r^2}$, therefore $v \simeq t - \frac{1}{r}$. Close to the event horizon located at $r = m^{1/d}$, $f'(r) \simeq \frac{1}{dm^{1/d}(r-m^{1/d}}$ with m the final black hole mass, $v \simeq t + \frac{1}{dm^{\frac{1}{d}}} log(r - m^{\frac{1}{d}})$. For this geometry to be a true thermal state at a finite boundary time t, $v \to -\infty$ and for finite v, $t \to \infty$.

The formation of the black hole may be characterised by the notion of trapped surfaces [8]. A trapped surface is a closed, spacelike surface where the expansion along future null directions is negative and the expansion along outgoing future null directions is zero. This can be quantified by the apparent horizon defined as the boundary of trapped surfaces for a given time foliation. The apparent horizon is located at $r_{AH} = (m(v))^{1/d}$. As can be seen in Fig.(7.2) the parameter a controls the gradient of the apparent horizon large a corresponds to large width of the mass shell in Fig.(7.1). The effect of the value of a for $d = 2, 3$ is shown in Fig.(7.2).

7.1 Quantum Quenches in AdS_3-Vaidya/CFT$_2$

Examining first the quantum quench in AdS_3/CFT$_2$, the AdS_3-Vaidya geometry models the CFT$_2$ being perturbed away from it's vacuum state at a boundary time $t = 0$. Since it models a CFT without a mass gap and thus an infinite correlation length, excitations may spread over the entire length of the system. In a CFT$_{1+1}$

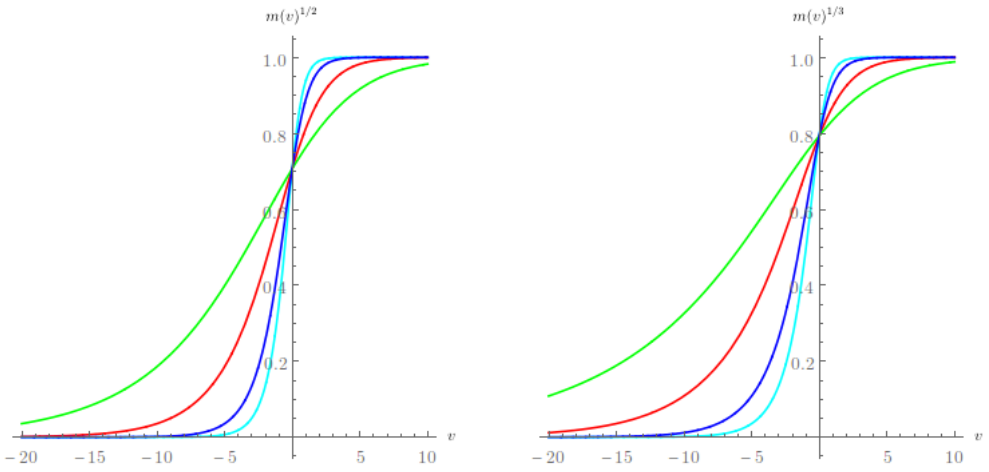

(a) (b)

Figure 7.2: Apparent horizon locations for $a = \frac{1}{3}, \frac{1}{2}, 1, 2$ in (a) AdS_3, and (b) AdS_4.

excitations may be either left or right moving and as the AdS_3-Vaidya geometry models the infall of matter along a lightcone coordinate both left and right moving excitations will spread over the system with velocity $v^2 = 1$, therefore after a time t, on $\mathbb{R}^{1,1}$, left and right moving excitations will be a distance $2t$ apart.

The entanglement entropy can be used to quantify the entanglement as the system evolves through time. Due to causality the perturbed system will never reach a true equilibrium at a global level, but locally the system will appear to be in equilibrium.

In Vaidya-AdS_3, for black hole formation stimulated by the collapse of matter in a smooth fashion, a true black hole can not form via this process in AdS space because in AdS the Page-Hawking phase transition separates AdS with in-falling matter from true black hole solutions [19], however, by picking a mass function $m(v)$ which smoothly interpolates between 0 and a final value m the process can approach, to within a good approximation, the BTZ black hole. The Vaidya-AdS_3 metric with final black hole temperature $T = \frac{\sqrt{m}}{2\pi}$ and boundary $\mathbb{R}^{1,1}$ is given by

$$ds^2 = -\left(r^2 - m(v)\right) dv^2 + 2dvdr + r^2 dx^2. \tag{7.4}$$

The mass function $m(v)$ should be picked to interpolate smoothly from 0 to m, the final black hole mass, therefore we take

$$m(v) = m\frac{\tanh\left(\frac{v}{a}\right) + 1}{2} \tag{7.5}$$

where the parameter a controls the extent of the perturbation, and thus this mass function models then CFT in its ground state for $t \lesssim -2a$, from then on the mass function begins to differ from 0. This choice of mass function interpolates from 0 to m in a time extent $\delta t \sim 4a$ whereby the mass function reaches $\sim 0.99m$ and the black hole can be considered formed, within a good approximation.

The metric (7.4) describes a CFT_2 dual with energy density and pressure

$$\epsilon = -\langle T_{tt}\rangle_{CFT} = \frac{m(t)}{16\pi G_N^{(3)}}, \tag{7.6}$$

$$p = \langle T_{xx}\rangle_{CFT} = \frac{m(t)}{16\pi G_N^{(3)}}. \tag{7.7}$$

which can be deduced in the same fashion as for the BTZ black hole in section (6) and a full derivation is given in Appendix (A).

To find the entanglement entropy in this system we must find the length of the geodesic which extends from a region of length ℓ on the boundary at a time t into the bulk of the Vaidya geometry. In [22] it was proposed that the prescription (5.1) can be also extended to dynamical, time evolving systems. As in (5.8) the length of the entangled region is ℓ. Parameterising with respect to the x coordinate the geodesic length may be obtained by minimising

$$L = \int_0^\ell \sqrt{r^2 + 2r'v' - (r^2 - m(v))v'^2}dx. \tag{7.8}$$

We have boundary conditions

$$r(0) = r(\ell) = \infty, \quad v(0) = v(\ell) = t \tag{7.9}$$

and we obtain the following equations of motion

$$2v'r' - \left(r^2 - m\left(v\right)\right)v'^2 - \frac{r^4}{r_0^2} = 0, \quad 2v'r' - r^2v'^2 - rv'' = 0. \tag{7.10}$$

where r_0, v_0 denotes the minimum values obtained by the geodesic in the coordinates r and v about which point the geodesics are symmetric. For $x \in [0, \ell]$ this point is located at $x = \frac{\ell}{2}$ where $r(\frac{\ell}{2}) = r_0$, $v(\frac{\ell}{2}) = v_0$ and $r'(\frac{\ell}{2}) = 0$, $v'(\frac{\ell}{2}) = 0$. Utilising this symmetry, combined with (7.10), the geodesic length (7.8) may be rewritten in a simplified form

$$L(\ell, t) = \frac{2}{r_0}\int_0^{\frac{\ell}{2}} r(x)^2 dx. \tag{7.11}$$

Applying (5.1) and (5.3) the entanglement entropy is

$$S(\ell, t) = \frac{c}{6}L(\ell, t) = \frac{c}{3r_0}\int_\delta^{\frac{\ell}{2}} r(x)^2 dx, \tag{7.12}$$

where the UV cutoff δ must be imposed close to the boundary. Near the boundary $r \to \infty$ the geodesics reduce to those on empty AdS_3 which obey the equations of motion (5.6), with $r = \frac{1}{z}$. Expanding near the boundary those geodesics behave as

$$x \simeq \frac{r_0}{2r^2}, \quad v \simeq t - \frac{1}{r} + \frac{b}{2r^2}. \tag{7.13}$$

For the case of empty AdS_3 and the BTZ black hole, the integration constant $b = 0$, however for the Vaidya solutions, in general $b = b(a, t, \ell) \neq 0$. In the neighbourhood of the endpoint located at $x = 0$ the boundary behaviour is

$$\begin{aligned} r &\simeq \sqrt{\frac{r_0}{2x}}, & v &\simeq t - \sqrt{\frac{2x}{r_0}} + \frac{bx}{r_0}, \\ r' &\simeq -\sqrt{\frac{r_0}{8}}x^{-\frac{3}{2}}, & v' &\simeq -\sqrt{\frac{1}{2xr_0}} + \frac{b}{r_0}. \end{aligned} \tag{7.14}$$

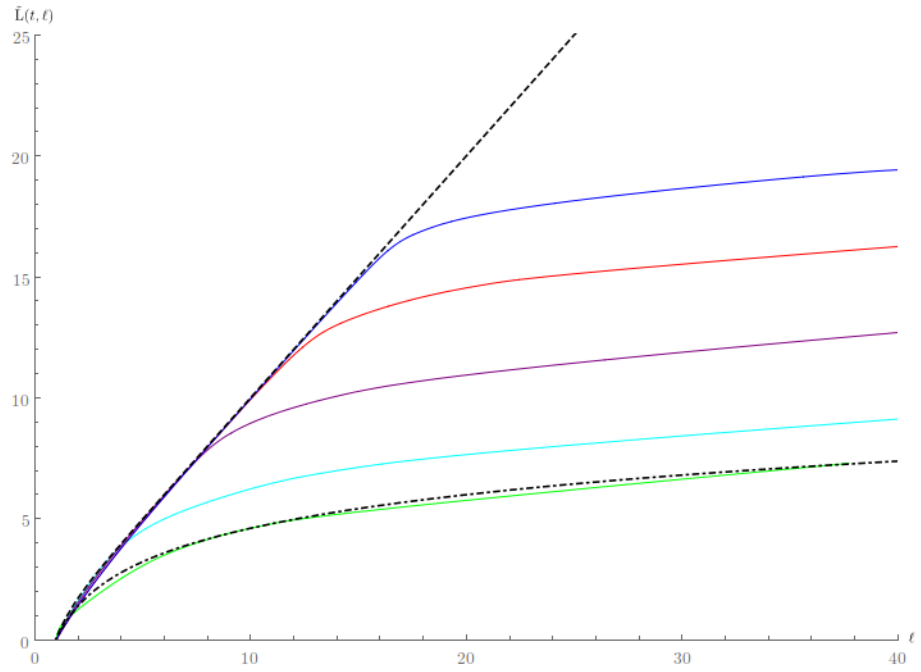

Figure 7.3: Plot of the UV independent part of the AdS_3-Vaidya geodesic length $\tilde{L}(t,\ell)$ against ℓ for $t = 0,2,4,6,8$ (bottom to top) the dot-dashed line represents the vacuum result and the dashed line the thermal result.

Equation (7.10) may be integrated with boundary conditions (7.9) and the boundary behaviour (7.14) to obtain numerical results for the geodesics. The holographic dictionary tells us that the relation between δ and the field theory UV cutoff ϵ is given by $\epsilon = \frac{1}{r(\delta)}$. The UV divergent independent part may be obtained by subtracting the UV divergent part of the vacuum result (5.8) from (7.12) to give

$$\tilde{S}(\ell,t) = \frac{c}{3}\tilde{L}(\ell,t) \tag{7.15}$$

$$= \frac{c}{3r_0}\int_{\delta}^{\frac{\ell}{2}} r(x)^2 dx - \frac{c}{3}\log\left(r(\delta)\right). \tag{7.16}$$

Fig.(7.3) shows the entanglement entropy as a function of ℓ for fixed t. For later values of t excitations may spread over larger and larger regions of the CFT requiring larger values of ℓ for the system to thermalise. At small values of $\ell \ll 1$, corresponding to r_0 staying close to the boundary, the entanglement entropy reproduces the logarithmic behaviour of the vacuum result (5.8) because for small values of ℓ the geodesics feel only an empty AdS_3 geometry. Moreover, for small values of t excitations will tend to spread only over short distances therefore the system is barely perturbed away from the vacuum result. As ℓ increases the geodesics feel the full dynamical Vaidya geometry resulting in a regime of linear growth proportional to $\frac{\ell}{\beta}$ which follows the thermal result (6.22). For values of $\ell \lesssim 2t$ the system begins to approach thermal equilibrium located at $\ell \simeq 2t$. For $\ell \gtrsim 2t$ the region of length $2t$ where excitations have spread may be regarded as a thermal state and the part of the CFT_2 outside this region follows the vacuum result, as indicated by the return to a logarithmic behaviour. This behaviour is illustrated in Fig.(7.5). Therefore, for large values of ℓ the effect of the perturbation can be described by an extensive,

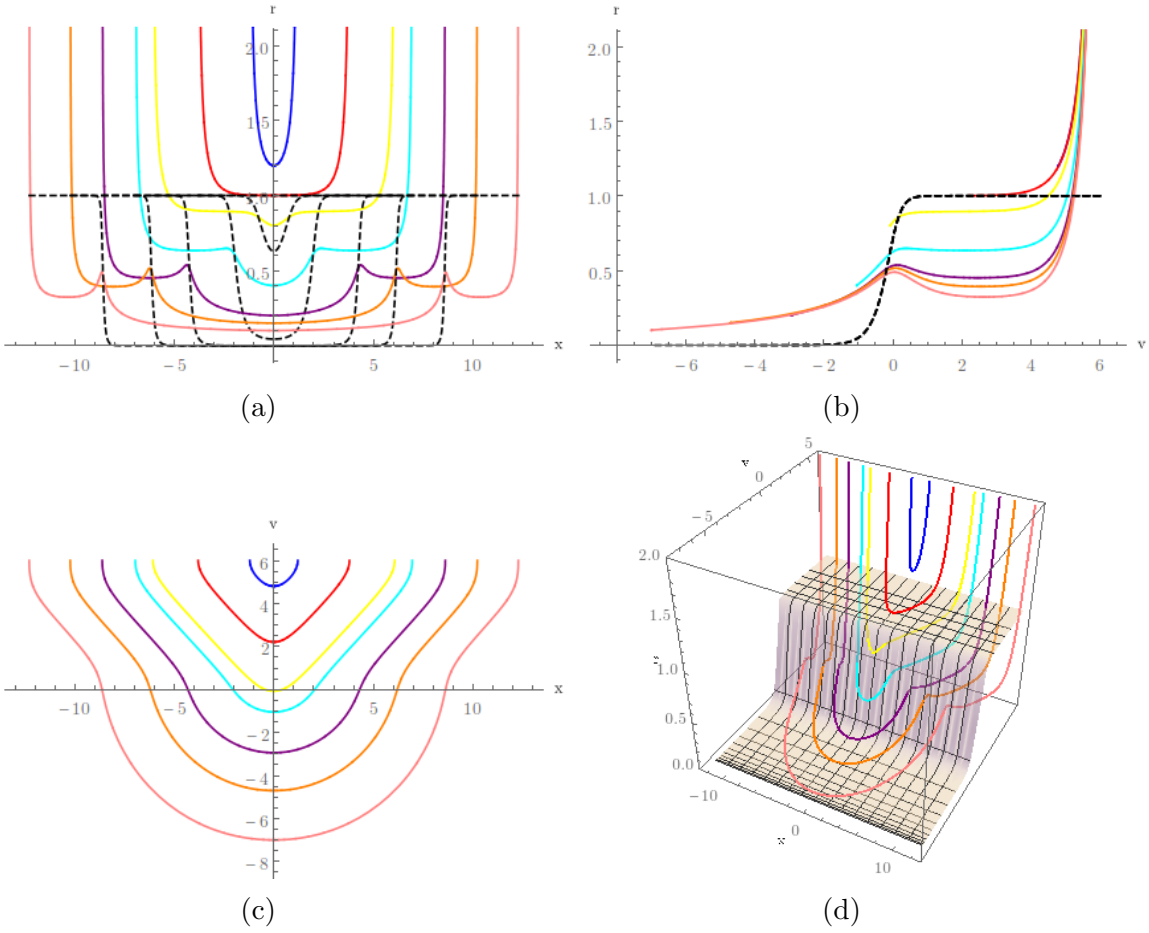

Figure 7.4: AdS_3-Vaidya Geodesics for $a = \frac{1}{3}$ and $t = 6$ for various ℓ : (a) r against x, (b) v against r, (c) v against x, (d) full geodesics in x,r,v. The dashed line in (a) and (b) and the solid surface in (d) represent the apparent horizon located at $m(v)^{\frac{1}{2}}$.

time dependent shift from the vacuum result

$$S(\ell, t) \to s(t) + \frac{c}{3} \log\left(\frac{\ell}{\epsilon}\right). \tag{7.17}$$

In terms of the geodesics as shown in Fig.(7.4) for values of ℓ corresponding to $r_0 \gtrsim 1$ the geodesics perceive a pure BTZ geometry yielding the linear behaviour in Fig.(7.3) for intermediate ℓ. As ℓ increases the geodesics feel the full Vaidya geometry and develop a dip around the midpoint $x = \frac{\ell}{2}$ which becomes more pronounced for large ℓ. The large ℓ geodesics pass through the apparent horizon where a metastable state in r develops inducing the extensive regime in the entanglement entropy. The geodesics then extend through the apparent horizon at approximately constant $r \simeq r_0$, in this regime the geodesics behave as those in pure AdS_3 and therefore the entanglement entropy manifests a logarithmic behaviour.

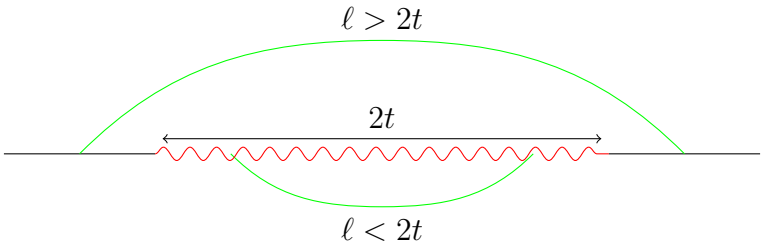

Figure 7.5: Illustration of the spread of excitations (wavy line) and the view of the entanglement entropy

In AdS_3 the coordinate v, by integrating $f(r)$ in (7.2) is given by

$$v = t - \frac{1}{2\sqrt{m}} \log\left(\frac{r+\sqrt{m}}{r-\sqrt{m}}\right) \tag{7.18}$$

and for the pure BTZ geometry the relation between ℓ and r_0 can be obtained from (6.18) to give

$$\ell = \frac{1}{\sqrt{m}} \log \frac{r_0+\sqrt{m}}{r_0-\sqrt{m}}. \tag{7.19}$$

Evaluating (7.18) and (7.19) at $v = v_0$, $r = r_0$ obtained at $x = \frac{\ell}{2}$ the pure BTZ geodesics satisfy the relation

$$\ell = 2(t - v_0) \tag{7.20}$$

and observing that, although strictly speaking the mass function (7.5) has non-compact support as $m(v) \neq 0 \ \forall \ v \in \mathbb{R}$ and $m(v)$ only reaches m asymptotically at $v = \infty$. The mass function (7.5) obtains a a value $m(v) \sim 0.98m$ at $v \sim 2a$. Therefore geodesics with $\ell \leq 2t - 4a$ will lie entirely within the BTZ geometry which agrees with the linear regime observed in Fig.(7.3). The UV independent part of (6.22) begins to become an extensive quantity at $\log\left(\sinh\left(\frac{\pi\ell}{\beta}\right)\right) \simeq \frac{2\pi\ell}{\beta} = \sqrt{m}\ell$ which requires $\ell \gtrsim \frac{\beta}{2}$. Then the bound $\ell \leq 2t - 4a$ dictates that extensive behaviour in the entanglement entropy is not exhibited before $t_0 \simeq \frac{\beta}{4} + 2a$ with $\beta = \frac{2\pi}{\sqrt{m}}$ explaining the vacuum like behaviour of the entanglement entropy observed in Fig.(7.3) before this time. Therefore for $\ell \simeq 2t - 4a + \delta t = 2t$ the entanglement entropy approaches thermal equilibrium. Equilibration does not reach regions of $\ell \gtrsim 2t$, for this the extensive part of the entanglement entropy saturates to a time dependent value which is independent of ℓ. Therefore we obtain the thermalisation time t_T for which an interval of length ℓ is at thermal equilibrium locally for $t \simeq t_T$

$$t_T \simeq \frac{\ell}{2}. \tag{7.21}$$

The physical reason for the thermal equilibrium behaviour for $\ell \simeq 2t$ is due to holomorphic factorisation. The AdS_3-Vaidya geometry models a CFT_2 undergoing a perturbation. The perturbation creates massless excitations which therefore travel at speed $v^2 = 1$. A CFT_2 admits holomorphic factorisation [36] meaning that left moving and right moving modes move away from each other and are non-interacting, with equal central charges $c_R = c_L = \frac{3R}{2G_N^{(3)}}$ [9]. Therefore after a time t excitations will have spread over a region of length $\zeta = \ell = 2t$, therefore for $\ell \gtrsim \zeta$

the entanglement entropy will perceive the region ζ to be at thermal equilibrium, inducing an extensive quantity to the entanglement entropy. Excitations will not have spread outside the region ζ where the CFT_2 will be in the vacuum state where the entanglement entropy scales logarithmically with ℓ.

The result (7.21) may have been completely determined from causality and the holomorphic dynamics of CFT_2, we conclude that the thermalisation behaviour is CFT_2 is trivial owing to the fact that excitations cannot interact, this leads us to look for a more interesting geometry which may model interactions between excitations.

7.2 Quantum Quenches for AdS_4-Vaidya/CFT_3

The AdS_3-Vaidya dual described in the previous section models a Quantum Quench on a CFT_2, this particular dual theory models a CFT_2 which admits holomorphic factorisation. Moreover, classical gravity in $d = 2 + 1$ is said to be "trivial", having no propagation of gravitational waves and no graviton as in $d = 2 + 1$ the Riemann curvature tensor $R_{\mu\nu\sigma\lambda}$ can be completely determined by the Ricci scalar R and the Ricci tensor $R_{\mu\nu}$, thus any solution of Einstein's equations has constant curvature $R_{\mu\nu} = 2\Lambda g_{\mu\nu}$ [12]. This reason leads us towards performing the analysis of a quantum quench on a CFT_3 via holographic techniques as due to the above mentioned reasons a CFT in $d = 2 + 1$ may exhibit additional behaviour in the entanglement entropy as CFT's in $d > 2$ do not, in general admit holomorphic factorisation.

This leads us towards evaluating a quantum quench modelled by a AdS_4-Vaidya/CFT_3 duality where the entangled region is an infinite strip of width ℓ and constant length $L \to \infty$. The analysis of this process is performed using largely the same techniques as implemented in Section (7.1) with the aim of finding a result for the thermalisation time $t_T = f(\ell, \beta)$ as in this case without holomorphic factorisation, the thermalisation time may exhibit additional temperature dependence which is notably absent from the CFT_2 thermalisation time (7.21).

The AdS_4-Vaidya metric is given by

$$ds^2 = -\left(r^2 - \frac{m(v)}{r}\right) dv^2 + 2drdv + r^2(dx^2 + dy^2). \tag{7.22}$$

This geometry (7.22) models a CFT_3 perturbed from its vacuum state at a time $t = 0$. The perturbations will spread entanglement over the entire y direction of length L for all t. As this models a CFT, conformal invariance would imply that excitations move at the speed of light $v^2 = 1$. Therefore for a given time t excitations will have spread, at most, over a region $\zeta \leq \ell L = 2tL$.

Using the prescription in [14] this describes a CFT_3 with energy density and pressure

$$\epsilon = -\langle T_{tt} \rangle_{CFT} = \frac{2m(t)}{16\pi G_N^{(4)}}, \tag{7.23}$$

$$p_{xx} = \langle T_{xx} \rangle_{CFT} = \frac{m(t)}{16\pi G_N^{(4)}}, \tag{7.24}$$

$$p_{yy} = \langle T_{yy} \rangle_{CFT} = \frac{m(t)}{16\pi G_N^{(4)}}, \tag{7.25}$$

as detailed in Appendix (B).

We have boundary conditions $r(0) = r(\ell) = \infty$, $v(0) = v(\ell) = t$. The area of the surface extending from the boundary into the AdS_4 bulk is given by

$$A(\beta, \ell) = \int_0^{\ell/2} \int_0^L \sqrt{g} dy dx = L \int_0^\ell \sqrt{r^2 \left(r^2 + 2r'v' - \left(r^2 - \frac{m(v)}{r} \right) v'^2 \right)} dx. \tag{7.26}$$

Minimising (7.26) we obtain the equations of motion

$$\frac{r^6}{r_0^4} = r^2 + 2r'v' - \left(r^2 - \frac{m(v)}{r} \right) v'^2, \quad 2v'' - \frac{r^5}{r_0^4} + \frac{6r'v'}{r} - 3r(v'^2 - 1). \tag{7.27}$$

Close to the boundary the behaviour of the surface reduces to that of the behaviour of the surface in empty AdS_4 described by (5.22)

$$x \simeq \frac{r_0^2}{3r^3}, \quad v \simeq t - \frac{1}{r} + \frac{b}{2r^2}. \tag{7.28}$$

In the neighbourhood of the $x = 0$ endpoint

$$\begin{aligned} r &\simeq \left(\frac{r_0^2}{3x} \right)^{\frac{1}{3}}, & v &\simeq t - \left(\frac{3x}{r_0^2} \right)^{\frac{1}{3}} + \frac{b}{2} \left(\frac{3x}{r_0^2} \right)^{\frac{2}{3}}, \\ r' &\simeq -\frac{1}{3} \left(\frac{r_0^2}{3x^4} \right)^{\frac{1}{3}}, & v' &\simeq -\frac{1}{3} \left(\frac{3}{r_0^2 x^2} \right)^{\frac{1}{3}} + \frac{b}{2} \left(\frac{3}{\sqrt{x} r_0^2} \right)^{\frac{2}{3}}. \end{aligned} \tag{7.29}$$

Using (7.27) and the symmetry of the surface about the points $v(\frac{\ell}{2}) = v_0$, $r(\frac{\ell}{2}) = r_0$ where $v'(\frac{\ell}{2}) = 0$ and $r'(\frac{\ell}{2}) = 0$, combined with (7.26) the entanglement entropy can be written as

$$S(\ell, t) = \frac{1}{4G_N^{(4)}} A(\ell, t) = \frac{2L}{4G_N^{(4)}} \int_\delta^{\frac{\ell}{2}} \frac{r(x)^4}{r_0^2} dx \tag{7.30}$$

with the UV cutoff δ imposed at $x \to 0$. Therefore the UV divergent independent part of the entanglement entropy is given by subtracting away the divergent part of (5.29) defined as

$$\tilde{S}(\ell, t) = \frac{1}{4G_N^{(4)}} \tilde{A}(\ell, t) = \frac{2L}{4G_N^{(4)}} \int_\delta^{\frac{\ell}{2}} \frac{r(x)^4}{r_0^2} dx - \frac{2L}{4G_N^{(4)}} r(\delta). \tag{7.31}$$

The vacuum result with which to compare this entanglement entropy is given by (5.29) for $d = 2$

$$S_{vac}(\ell) = \frac{1}{4G_N^{(4)}} \left[2 \left(\frac{L}{\epsilon} \right) - 4\pi \left(\frac{\Gamma(\frac{3}{4})}{\Gamma(\frac{1}{4})} \right)^2 \left(\frac{L}{\ell} \right) \right]. \tag{7.32}$$

Then the UV independent part of the vacuum result $\tilde{S}_{Vac}(\ell)$ is given by

$$\tilde{S}_{vac}(\ell) = \frac{1}{4G_N^{(4)}} \left[-4\pi \left(\frac{\Gamma(\frac{3}{4})}{\Gamma(\frac{1}{4})} \right)^2 \left(\frac{L}{\ell} \right) \right]. \tag{7.33}$$

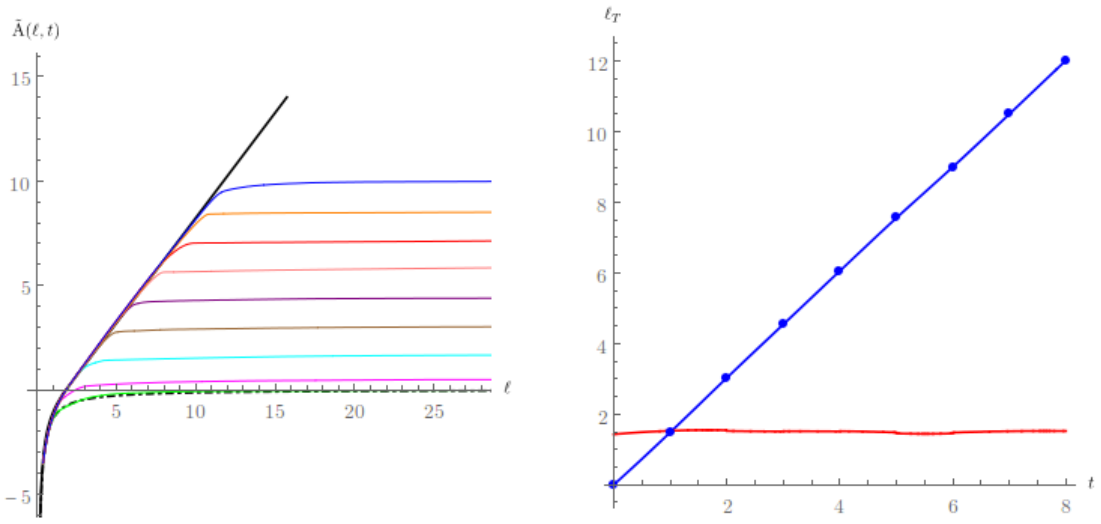

(a) (b)

Figure 7.6: (a) Plot of the UV independent part of the AdS_4-Vaidya minimal surface area $\tilde{A}(t,\ell)$ against ℓ for $a = \frac{1}{3}$ and t = 0,1,..,8 (bottom to top) the dashed line represents the vacuum result and the solid black line the thermal result. (b) Plot of thermalisation length ℓ_T as a function of t and its derivative $\frac{d\ell_T}{dt}$.

We note that although the UV independent part of the vacuum result $\tilde{S}_{vac}(\ell) \lesssim 0$ for all values of ℓ, however the full UV dependent part of the entanglement entropy $S_{vac}(\ell) \geq 0$ for all ℓ.

Unlike in the BTZ/CFT$_2$ case an analytical result for the entanglement entropy of a infinite strip for AdS_4-Schwarzschild/CFT$_3$ with the CFT at inverse temperature β is hard to obtain. We require at least a numerical result to allow us to infer thermalisation times in the CFT$_3$ quantum quench. The dual to a CFT$_3$ at inverse temperature $\beta = \frac{2\pi}{\sqrt{m}}$ is given by the AdS_4-Schwarzschild black hole

$$ds^2 = -\left(r^2 - \frac{m}{r}\right)dt^2 + \left(\frac{dr^2}{r^2 - \frac{m}{r}}\right) + r^2(dx^2 + dy^2). \tag{7.34}$$

The area of the minimal surface γ_A extending from the boundary region of length L and width ℓ is given by

$$Area(\gamma_A) = \int \sqrt{g|_{ind}}drdy = 2L\int_0^{\frac{\ell}{2}} \sqrt{\frac{r^2}{r^2 - \frac{m}{r}} + r^4 x'^2}dr. \tag{7.35}$$

Yielding the equation of motion

$$x'(r) = \sqrt{\frac{r_0^4}{r^2(r^2 - \frac{m}{r})(r^4 - r_0^4)}}. \tag{7.36}$$

This must be integrated with boundary conditions $x(\infty) = 0$, $x(r_0) = \frac{\ell}{2}$. Imposing a UV cutoff δ close the boundary near the endpoint $x = 0$ the UV independent part of the entanglement entropy is then

$$\tilde{S}_\beta(\ell,\beta) = \frac{2L}{4G_N^{(4)}}\int_\delta^{\frac{\ell}{2}} \sqrt{\frac{r^6}{(r^2 - \frac{m}{r})(r^4 - r_0^4)}} - \frac{2L}{4G_N^{(4)}}r(\delta). \tag{7.37}$$

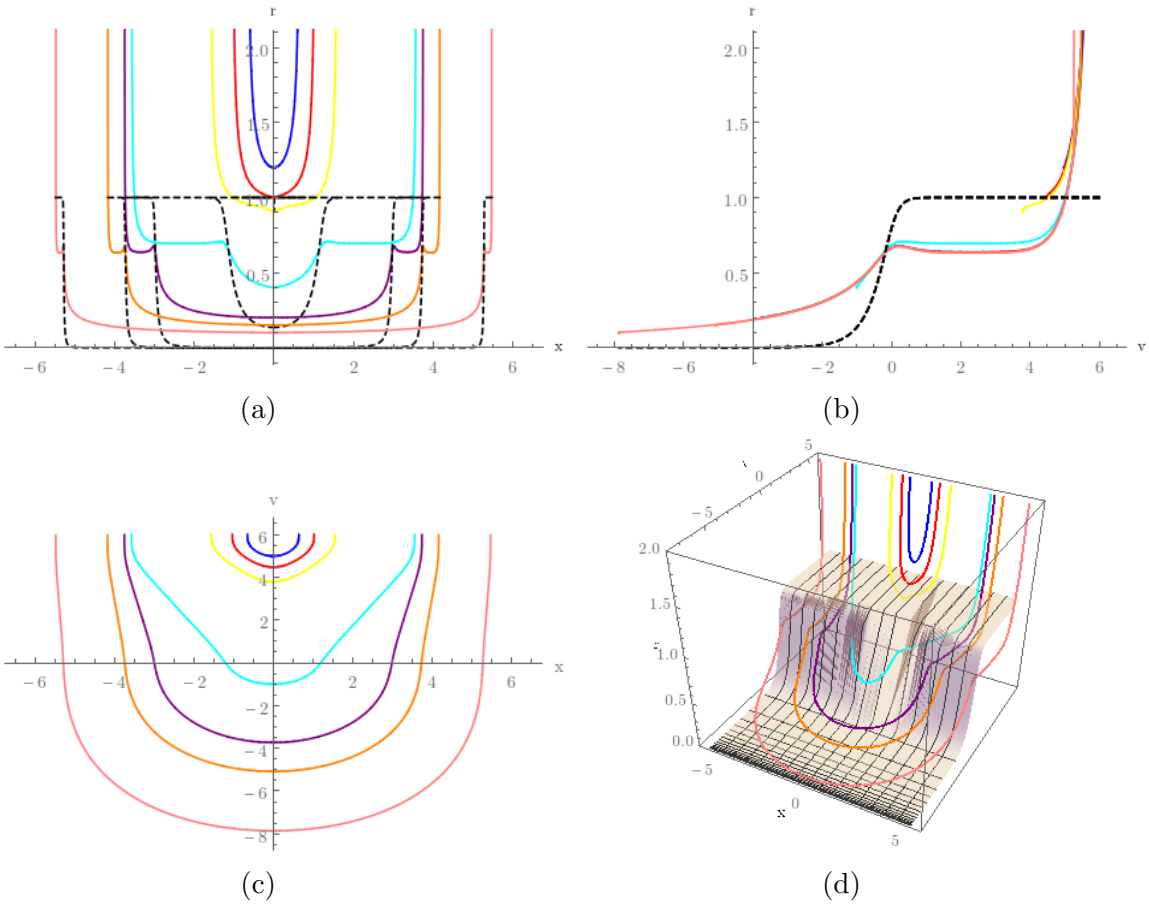

Figure 7.7: AdS_4-Vaidya minimal surface cross sections for $a = \frac{1}{3}$ and $t = 6$ for various ℓ projected in the : (a) r, x plane; (b) v ,r plane; (c) v, x plane; (d) x,r,v plane. The dashed line in (a) and (b) and the solid surface in (d) represents the position of the apparent horizon located at $m(v)^{\frac{1}{3}}$.

Performing the numerical integration on (7.26), (7.27) and (7.29) where, for simplicity, we set $L = 1$ which can be easily reintroduced by sending $A(\ell, t) \to LA(\ell, t)$ as L is simply a large multiplicative constant. As shown in Fig.(7.6a) we obtain a visually similar picture to result obtained in Section (7.1) for the AdS_3-Vaidya/CFT$_2$ case.

For small ℓ where the thermal result is not yet in a linear regime $\tilde{S}_\beta(\ell, \beta) \lesssim 0$ the entanglement entropy behaves like the vacuum result proportional to $-\frac{1}{\ell}$. For intermediate values of ℓ the entanglement entropy exhibits a regime of linear growth described by $\sqrt{m}\ell = \frac{2\pi}{\beta}\ell$ following very closely the entanglement entropy behaviour of the thermal AdS_4-Schwarzschild/CFT$_3$ result. This linear regime comes to an end for $\ell \simeq 1.5t$. For values of $\ell \gtrsim 1.5t$ the entanglement entropy saturates to approximately a constant value from then on, as in the CFT$_2$ case, the entanglement entropy can , from then on, be described by a time dependent shift from the vacuum result (7.32) described by

$$S(\ell, t) = s(t)L + S_{vac}(\ell) \tag{7.38}$$

$$= s(t)L + \frac{1}{4G_N^{(4)}}\left[2\left(\frac{L}{\epsilon}\right) - 4\pi\left(\frac{\Gamma(\frac{3}{4})}{\Gamma(\frac{1}{4})}\right)^2\left(\frac{L}{\ell}\right)\right]. \tag{7.39}$$

Fig.(7.6b) shows a plot of the thermalisation length for which $\ell \simeq \ell_T(t)$ the system appears to be in thermal equilibrium and the entanglement entropy behaves as an extensive quantity. We find, from Fig.(7.6b) $\frac{d\ell_T(t)}{dt} \simeq \frac{3}{2}$. Thus we numerically identify the thermalisation time t_T for which a strip of CFT_3 of width ℓ and length L is at local equilibrium

$$t_T = f(\ell, \beta) \simeq \frac{2}{3}\ell. \tag{7.40}$$

t_T clearly scales linearly with ℓ and dimensional analysis would imply that this result is in fact independent of β. One would possibly entertain the idea of involving a β dependence by building a dimensionless quantity involving L and β, e.g. $\frac{\beta}{L}$, but we would infer that t_T cannot have any L dependence as we are free to choose L without altering the value of t_T and L only scales the entanglement entropy by a constant multiple.

In terms of the minimal surface cross sections in Fig.(7.7) for small ℓ, before entering the full Vaidya geometry, the 2-dimensional cross-sections of the surfaces are very similar to the geodesics for the CFT_2 in Fig.(7.4). When the surface enters the dynamical Vaidya geometry some differences appear. In Fig.(7.7a) we see that as ℓ increases the surfaces can cross the apparent horizon for $v > 0$, this dip appears even for $r_0 \lesssim 1$. From there on a metastable dip in r develops behind the apparent horizon. As ℓ increases the piece behind the apparent horizon in the r-x plane decreases and begins to wrap around the apparent horizon where in this region the gradients $\frac{dr}{dx} \to -\infty$, $\frac{dv}{dx} \to -\infty$ in the limit $\ell \to \infty$. An interpretation of this is given in Section (7.3). The part of the surface coming after the dip in the apparent horizon extends at approximately constant r and behaves like a large ℓ surface in AdS_4 close to $r_0 \gtrsim 0$. The picture in the r-v looks largely similar to the CFT_2 picture Fig.(7.4b) however a surface in this plane may extend through the apparent horizon without necessarily leaving it.

Recalling the relation for the maximum area ζ that excitations with velocity $v^2 = 1$ may spread over $\zeta \leq \ell L = 2tL$, due to causality. For t_T (7.40) in we find that quantity

$$2t_T L = \frac{4}{3}\ell L > \zeta. \tag{7.41}$$

This implies that, due to causality, there must be some interactions between excitations created by perturbations in a CFT_3 and these excitations cannot be holomorphically factorised and are therefore less trivial than in the CFT_2 case which is decided entirely by (1+1)-dimensional conformal kinematics.

7.3 Behaviour near the Apparent Horizon

As shown in the previous two sections the minimal surfaces in both AdS_3-Vaidya and AdS_4-Vaidya can cross behind the apparent horizon. The piece behind the apparent horizon, where the geodesics develop a dip, extends over a region of length Δx between the point where the position of the apparent horizon sharply drops to zero, denoted by x_{AH} and $\frac{\ell}{2}$ in Figures (7.4a) and (7.7a). Note that for the AdS_3-Vaidya geometry at large ℓ this length Δx tends to a constant. For the AdS_3-Vaidya geometry, in the r-x plane Fig.(7.4a) for small ℓ the geodesics do not feel the full effect of the perturbation induced by the Vaidya geometry and thus are barely perturbed from the vacuum state. For large ℓ the geodesics feel the full effect of

the perturbation the length of the piece behind the apparent horizon saturates to approximately a constant value for $\ell \to \infty$. On the contrary, in AdS_4-Vaidya as ℓ becomes large the length of Δx decreases and the surface tends to shift towards wrapping around the apparent horizon and the gradients in the dip become very sharp. So

$$\begin{cases} \lim_{\ell\to\infty} \Delta x \to const & AdS_3\text{-Vaidya} \\ \lim_{\ell\to\infty} \Delta x \to 0 & AdS_4\text{-Vaidya.} \end{cases}$$

The difference in behaviour of Fig.(7.4a) and Fig.(7.7a) close to the point x_{AH} can be understood by examining the actions close to this point.

Examining the action of the AdS_3-Vaidya action (7.8) at large values of ℓ in the region Δx

$$L(\ell, t) \to 2 \int_{x_{AH}}^{\ell/2} \sqrt{r^2 + 2r'v' - (r^2 - m(v))v'^2} dx. \tag{7.42}$$

$r(x_{AH}) \ll 1$ so the action in this region will be finite and non-zero as required provided $\frac{dr}{dx}|_{x_{AH}} \to A$, $\frac{dv}{dx}|_{x_{AH}} \to B$, with A, B constants.

Comparing to the AdS_4-Vaidya case we see that in this same region Δx tends to zero for large values of ℓ as can be seen in Fig.(7.7a) as the dip in region tends to become very sharp and the values x_{AH} and $\frac{\ell}{2}$ tend to coincide. The action is

$$A(\ell, t) \to 2L \int_{x_{AH}}^{\ell/2} \sqrt{r^2(r^2 + 2r'v' - (r^2 - m(v))v'^2)} dx \tag{7.43}$$

$r(x_{AH}) \ll 1$ then close the point x_{AH} to ensure a finite, non-vanishing action at this point the values of the gradients must $\frac{dr}{dx}|_{x_{AH}} \to \infty$, $\frac{dv}{dx}|_{x_{AH}} \to \infty$. This explains the sharp behaviour in the AdS_4-Vaidya surfaces close to the apparent horizon for large ℓ.

Chapter 8

Discussion

The entanglement entropy has been obtained from the AdS/CFT correspondence from the prescription [31] and the entanglement entropy for a CFT_2 matches results found in [21, 11] and goes as the logarithm of the length $S = \frac{c}{3}\log\frac{\ell}{\epsilon}$. Although the prescription has not yet been proven, it agrees with many result, specifically for 2-dimensional CFT's. A full proof of the entanglement entropy prescription would require a bulk-to -boundary derivation similar to those in section (4).

It is also shown in section (5) that the minimal surfaces in the entanglement entropy calculation may imply the presence of a confinement/deconfinement phase transition, and in [24] it was shown that this may be applied to more interesting geometries which describe dual field theories which contain more interesting features than those dual to empty AdS.

The prescription can be applied to calculate entanglement entropy's of thermal CFT's. The dual to a thermal CFT is given by a black hole in AdS space. The prescription can also be applied to dynamical systems. We have applied this to the process of a CFT undergoing a quantum quench, the dual theory is given by Vaidya solutions. For a CFT_2 result were found which follow very closely the analytical results found in [10] of $t_T \simeq \frac{\ell}{2}$. The process was also applied to a higher dimensional CFT_3, in this regime analytical results are hard to come by, but holography provides us with a powerful tool to observe the behaviour of the entanglement entropy of a many body quantum system where results via traditional methods would be significantly harder to obtain. We obtain $t_T \simeq \frac{2\ell}{3}$.

In [1] is was left as a somewhat open question as to the physical interpretation of the apparent horizon in the context of entanglement entropy and minimal surfaces in the AdS/CFT correspondence. An interesting question to ask is the role of the Apparent horizon in terms of the dual CFT. The difference in behaviour of minimal surfaces near the apparent horizon in the holographic CFT_2 and CFT_3 duals may possibly be interpreted in terms of some hidden information. The piece behind the apparent horizon, for large ℓ, contributes the extensive part $s(t)$ to the entanglement entropy. For a CFT_2 the piece behind the apparent horizon remains constant in the r-x plane for large ℓ and for a CFT_3 the piece behind the apparent horizon in the x coordinate tends to zero for large ℓ and this piece of the surface begins to wrap around the apparent horizon. We have demonstrated that left and right moving excitations are non-interacting thus it would that excitations in the left-moving and right-moving regimes have no knowledge of the thermalisation behaviour of one another, this could possibly explain the constant part of the entanglement entropy

remaining behind the apparent horizon, smearing out the thermalisation behaviour from left and right movers.

For CFT_3 excitations interact thus as ℓ increases the entanglement entropy has access to the excitations. As the interactions interact, as the system relaxes from the effect of the perturbation the excitations can be in causal contact with one another thus the part of the surface smeared out behind apparent horizon becomes smaller as ℓ increases.

In the future it would be very interesting to investigate the thermalisation behaviour in CFT's with dimension greater than three. We are lead to this because for a CFT_2 we see $t_T \approx \frac{1}{2}\ell$ and for a CFT_3 $t_T \approx \frac{2}{3}\ell$ which may imply a possible scaling relation $t_T \approx \frac{d-1}{d}\ell$ which could be numerically tested and we would like to check the behaviour of t_T in the large d limit.

Moreover, we would like to investigate the CFT quantum quench process with an AdS-Vaidya duality when the AdS boundary is compactified, for example AdS_3-Vaidya with $\mathbf{S}^1$ boundary. Thermalisation in this geometry may give interesting behaviour due to the periodicity in the time-like coordinate imposed on AdS as discussed in section (6).

In conclusion it has been demonstrated that the entanglement entropy provides a powerful tool with which to probe strongly coupled, many-body quantum systems. The simple interpretation in terms of holography provides us with a simple way with which to obtain entanglement entropy's in systems which would otherwise be too complex to obtain meaningful results.

On the other hand the entanglement entropy is, in some ways, too simplistic of an observable to gain specific details of the boundary field theory and it tends to hide interesting properties such as details of the interactions. This would lead us to consider more exotic forms of the entanglement entropy. One such quantity which could be considered is the mutual information. The mutual information measures the information shared by two systems A and B. The mutual information may be derived from the entanglement entropy. For two intervals A and B the mutual information is given by [17]

$$I(A,B) = S_A + S_B - S_{A\cup B}. \tag{8.1}$$

The mutual information is a more sophisticated measure of entanglement and details the entanglement between two systems in a way that is free of UV divergences. It would be interesting to investigate the behaviour of the mutual information in the quantum quench process.

Appendix A

Fefferman-Graham expansion of Vaidya-AdS$_3$

The Vaiyda-AdS$_3$ metric is given by

$$ds^2 = -(r^2 - m(v))dv^2 + 2dvdr + r^2dx^2. \tag{A.1}$$

To calculate the CFT$_2$ stress tensor [14] the metric must be cast into Fefferman-Graham form [15, 16]

$$ds^2 = \frac{R^2}{\rho^2}\left(d\rho^2 + g_{ij}(x,\rho)dx^i dx^j\right) \tag{A.2}$$

where $g_{ij} = g_{ij}^{(0)} + g_{ij}^{(2)}\rho^2 + ... + g_{ij}^{(d)}\rho^d + ...$, where d is the CFT dimension. Then the CFT stress energy tensor components are given by

$$\langle T_{ij}\rangle_{CFT} = \frac{dR^{d-1}}{16\pi G_N^{(d+1)}} g_{ij}^{(d)} + X_{ij}[g^n] \tag{A.3}$$

where $X_{ij}[g^n]$ is a function of the FG metric for $n < d$ and reflects the conformal anomaly in even d systems. For $d = 2$ [14]

$$\langle T_{ij}\rangle_{CFT} = \frac{2R}{16\pi G_N^{(3)}}\left(g_{ij}^{(2)} - g_{ij}^{(0)}\,\mathrm{Tr}\,(g_{ij}^{(2)})\right). \tag{A.4}$$

First we must undo the Vaidya transformation (A.1) and asymptotically cast the metric in Schwarzchild-like form. We make the transformation $v = t + f(t,r)$ and we wish to pick $f(t,r)$ such that the $drdt$ terms vanish. A closed form of $f(t,r)$ is hard to find. The behaviour of v close to the boundary $r \to \infty$ is known $v \approx t - \frac{1}{r} + ...$ where we also note that in this limit $m(v) \to m(t)$. This leads us to the asymptotic expansion of $f(t,r)$

$$f(t,r) = \sum_{n=1} \frac{c_n(t)}{r^n} \tag{A.5}$$

$$\approx -\frac{1}{r} + \frac{c_2(t)}{r^2} + \frac{c_3(t)}{r^3} + ... \tag{A.6}$$

Subbing into (A.1) we find the $drdt$ coefficient, to leading order and setting equal to zero

$$0 = \frac{4c_2(t)}{r} + \frac{6c_3(t)}{r^2} + \frac{2m(t)}{r^2} - \frac{4c_2(t)m(t)}{r^3} + ... \tag{A.7}$$

thus we deduce that $f(t,r)$ must contain only odd powers of r and $c_3(t) = \frac{m(t)}{3}$. Subbing $f(t,r)$, up to $O(r^{-3})$, into (A.1)

$$ds^2 = -\left(r^2 - m(t)\right)dt^2 + \left(\frac{1}{r^2} + \frac{m(t)}{r^4} + \frac{m(t)^2}{r^6} + ...\right)dr^2 + r^2dx^2 \tag{A.8}$$

$$= -\left(r^2 - m(t)\right)dt^2 + \left(\frac{1}{r^2 - m(t)}\right)dr^2 + r^2dx^2. \tag{A.9}$$

The metric has been cast in a Schwarzchild-like form which is valid in the asymptotic limit $r \to \infty$. To place this metric into Fefferman-Graham form we make the substitution

$$\int \frac{d\rho}{\rho} = \int \frac{dr}{\sqrt{r^2 - m(t)}} \tag{A.10}$$

$$\rho = A(r + \sqrt{r^2 - m(t)}) \tag{A.11}$$

picking $A = \frac{2}{m(t)}$ so that for $r \to \infty$, $\rho \to \frac{1}{r}$, then

$$r = \frac{1}{\rho} + \frac{m(t)\rho}{4}, \tag{A.12}$$

in this choice of Fefferman-Graham coordinates the boundary is located at $\rho = 0$. Subbing in to r

$$ds^2 = \frac{1}{\rho^2}\left(d\rho^2 - \left(1 - \frac{m\rho^2}{2} + \frac{m(t)^2\rho^4}{16}\right)dt^2 + \left(1 + \frac{m\rho^2}{2} + \frac{m(t)^2\rho^4}{16}\right)dx^2\right). \tag{A.13}$$

Asymptotically $\rho \to 0$ the metric has the form of flat Minkowski space $ds^2 \to -dt^2 + dx^2$. Applying (A.4) and noting that $\mathrm{Tr}\,(g^{(2)}_{ij}) = 0$, we obtain the Vaidya-$AdS_3$ dual CFT_2 stress-energy tensor

$$\langle T_{ij}\rangle_{CFT} = \frac{1}{16\pi G_N^{(3)}}\begin{pmatrix} -m(t) & 0 \\ 0 & m(t) \end{pmatrix}. \tag{A.14}$$

Giving the pressure and energy density

$$\epsilon = -\langle T_{tt}\rangle_{CFT} = \frac{m(t)}{16\pi G_N^{(3)}} \tag{A.15}$$

$$p = \langle T_{xx}\rangle_{CFT} = \frac{m(t)}{16\pi G_N^{(3)}}. \tag{A.16}$$

Appendix B

Fefferman-Graham expansion of Vaidya-AdS$_4$

We wish to cast the Vaidya-AdS$_4$ metric in Fefferman-Graham form [15, 16]

$$ds^2 = \frac{R^2}{\rho^2}\left(d\rho^2 + g_{ij}(x,\rho)dx^i dx^j\right) \tag{B.1}$$

to obtain the CFT stress energy tensor $\langle T_{ij}\rangle_{CFT}$. Setting the curvature radius $R = 1$ the Vaidya-AdS$_4$ metric is given by

$$ds^2 = -\left(r^2 - \frac{m(v)}{r}\right)dv^2 + 2drdv + r^2(dx^2 + dy^2). \tag{B.2}$$

which can be cast in Schwarzchild-like coordinates in a similar fashion as in Appendix A with the transformation $v = t + f(t,r)$ where we construct $f(t,r)$ as an asymptotic expansion near the boundary $r \to \infty$, $v \approx t - \frac{1}{r} + ...$ in this limit $m(v) \approx m(t)$

$$f(t,r) = \sum_{n=1} \frac{c_n(t)}{r^n} \tag{B.3}$$

$$\approx -\frac{1}{r} + \frac{c_2(t)}{r^2} + \frac{c_3(t)}{r^3} + \frac{c_4(t)}{r^4} + ... \quad . \tag{B.4}$$

Subbing in to (B) and choosing $f(t,r)$ such that the $dtdr$ coefficient vanishes we find

$$c_2(t) = 0 \tag{B.5}$$

$$c_3(t) = 0 \tag{B.6}$$

$$c_4(t) = -\frac{m(t)}{4}. \tag{B.7}$$

this gives the dr^2 term of the metric

$$g_{rr} \approx \frac{1}{r^2} + \frac{m(t)}{r^5} + \frac{m(t)^2}{r^8} + \frac{m(t)^3}{r^{11}} + ... \tag{B.8}$$

$$= \frac{1}{r^2 - \frac{m(t)}{r}}. \tag{B.9}$$

Which gives the metric in Schwarzchild form

$$ds^2 = -(r^2 - \frac{m(t)}{r})dt^2 + \frac{dr}{r^2 - \frac{m(t)}{r}} + r^2(dx^2 + dy^2). \tag{B.10}$$

To cast the metric in FG form we make the transformation $\frac{dr}{\sqrt{r^2 - \frac{m(t)}{r}}} = -\frac{d\rho}{\rho}$. Integrating we obtain

$$\log \rho = \int \frac{dr}{\sqrt{r^2 - \frac{m(t)}{r}}} \tag{B.11}$$

$$\rho = \left(\frac{A}{m}\left(r^{\frac{3}{2}} - \sqrt{r^3 - m(t)}\right)\right)^{\frac{2}{3}} \tag{B.12}$$

asymptotically, as $r \to \infty$, $\rho \to \frac{A^{2/3}}{2^{2/3}r} + \frac{A^{2/3}m(t)}{6\times 2^{2/3}r^4} + ...$ Thus we pick the constant A such that $\rho \to \frac{1}{r}$ so $A = 2$. Rearranging (B.12) we find

$$r = \frac{(1 + \frac{m(t)\rho^3}{4})^{\frac{2}{3}}}{\rho} \tag{B.13}$$

which gives the metric in FG form

$$ds^2 = \frac{1}{\rho^2}\left(d\rho^2 - \left(\left(1 + \frac{m(t)\rho^3}{4}\right)^{\frac{4}{3}} - \frac{m(t)\rho^3}{1 + \frac{m(t)\rho^3}{4}}\right)dt^2 + \left(1 + \frac{m(t)\rho^3}{4}\right)^{\frac{4}{3}}(dx^2 + dy^2)\right). \tag{B.14}$$

The CFT$_d$ stress energy tensor is then given by [14]

$$\langle T_{ij}\rangle_{CFT} = \frac{dR^{d-1}}{16\pi G_N^{(d+1)}} g_{ij}^{(d)} + X_{ij}[g^n] \tag{B.15}$$

For odd d there are no conformal anomalies thus the term $X_{ij}[g^n]$ vanishes. Asymptotically expanding the dt, dx and dy around $\rho \to 0$ we find

$$g_{tt} = -1 + \frac{2m(t)\rho^3}{3} - \frac{13m(t)^2\rho^6}{72} + \frac{23m(t)^3\rho^9}{648} + O(\rho^{11}), \tag{B.16}$$

$$g_{xx} = 1 + \frac{m(t)\rho^3}{3} + \frac{m(t)^2\rho^6}{72} - \frac{m(t)^3\rho^9}{1296} + O(\rho^{11}), \tag{B.17}$$

$$g_{yy} = 1 + \frac{m(t)\rho^3}{3} + \frac{m(t)^2\rho^6}{72} - \frac{m(t)^3\rho^9}{1296} + O(\rho^{11}). \tag{B.18}$$

In the limit $\rho \to 0$ the metric tends to a flat M^3 boundary $ds^2 \to -dt^2 + dx^2 + dy^2$. Taking up to order $g_{ij}^{(3)}$ as indicated in (B.15) near the boundary we obtain

$$ds^2 = \left[\frac{1}{\rho^2}\left(d\rho^2 - \left(1 - \frac{2m(t)\rho^3}{3} + ...\right)dt^2 + \left(1 + \frac{m(t)\rho^3}{3} + ...\right)(dx^2 + dy^2)\right)\right]. \tag{B.19}$$

Applying (B.15) we find

$$\langle T_{ij}\rangle_{CFT} = \frac{3}{16\pi G_N^{(4)}}\begin{pmatrix} -\frac{2m(t)}{3} & 0 & 0 \\ 0 & \frac{m(t)}{3} & 0 \\ 0 & 0 & \frac{m(t)}{3} \end{pmatrix} \tag{B.20}$$

which gives $\langle T_i^i \rangle_{CFT} = 0$ as expected for a CFT. Giving the CFT energy density ϵ and pressure p

$$\epsilon = -\langle T_{tt} \rangle_{CFT} = \frac{m(t)}{8\pi G_N^{(4)}} \tag{B.21}$$

$$p_{xx} = \langle T_{xx} \rangle_{CFT} = \frac{m(t)}{16\pi G_N^{(4)}} \tag{B.22}$$

$$p_{yy} = \langle T_{yy} \rangle_{CFT} = \frac{m(t)}{16\pi G_N^{(4)}}. \tag{B.23}$$

Appendix C

Mathematica code for Vaidya-(AdS_3/AdS_4)

Below is the main *Mathematica 10* function used to generate the Vaidya-AdS_3 results. This function does the following: takes arguments r0,t,b,Col, where Col defines the line colour of the output figures. 1. Produce a inital solution Sol to calculate l/2 2. Produce SolL, i.e. the solution for v,r running from -l/2 to -x0 3. Returns in order: (1-3) plots of the geodesics in the rx,vx,rv planes, (4) the value of ℓ, (5) Geodesic Length, (5) surface plot in x,v,r and (7) apparent horizon in x,v,r. The plots produced from 3. may be reflected to give the full plots for $x \in [-\frac{\ell}{2}, \frac{\ell}{2}]$.

```
f[r0_,t_,b_,Col_]:=Module[{a,m0,Eqn1,Eqn2,r,x,v,rmax,xmax,x0,Sol,l,SolL
    ,gr1,gr2,gr3,LInt,dot,scal,gr4,temp1,AH,y},
     a=1/3;
     m0=1;
     m[v_]:=m0 (Tanh[v/a]+1)/2;
     Eqn1=r0^2 (r[x]^2+2r'[x]v'[x]-(r[x]^2-m[v[x]])v'[x]^2)-r[x]^4;
     Eqn2=r[x]^2-r[x]^2 v'[x]^2-r[x]v''[x]+2v'[x]r'[x];
     rmax=100;
     x0=r0/(2(rmax)^2);
     xmax=100;

     Sol=NDSolve[{Eqn1==0,Eqn2==0,r[x0]==rmax,v[x0]==t,v'[x0]==-(rmax
         /r0)+b/r0},{r,v},{x,x0,xmax}];

     l=2*x/.Last[Quiet[FindMinimum[v[x]/.Sol,{x,x0,x0,xmax}]]];

     SolL=NDSolve[{Eqn1==0,Eqn2==0,r[-l/2]==rmax,v[-l/2]==t,v'[-l/2]==
         =-(rmax/r0)+b/r0},{r,v},{x,-l/2,-x0},"ExtrapolationHandler
         "->{Indeterminate &}];

     gr1=Plot[{Evaluate[r[x]/.SolL],Evaluate[Sqrt[m[v[x]]]/.SolL]},{x
         ,-l/2,l/2},PlotStyle->{Col,{Dashed,Black}},PlotRange->All];

     gr2=Plot[Evaluate[v[x]/.SolL],{x,-l/2,l/2},PlotStyle->{Col},Plot
         Range->All];

     gr3=ParametricPlot[{Evaluate[{v[x],r[x]}/.SolL],Evaluate[{v[x],S
         qrt[m[v[x]]]}/.SolL]},{x,-l/2,-x0},AspectRatio->1/GoldenRati
         o,PlotRange->All,PlotStyle->{Col,{Black,Dashed}}];

     LInt=2/r0*(NIntegrate[r[x]^2/.SolL,{x,-l/2,-x0}])-2Log[r[-l/2]/.
```

```
            SolL[[1]]];

    gr4=ParametricPlot3D[Evaluate[{x,v[x],r[x]}/.SolL],{x,-(l/2),-x0
        },PlotRange->All,PlotStyle->Col];

    AH=ParametricPlot3D[Evaluate[{y,v[x],Sqrt[m[v[x]]]}/.SolL],{x,-(
        l/2),-x0},{y,-(l/2),l/2},PlotRange->All,PlotStyle->{LightBlue
        ,Opacity[0.5]}];
{gr1,gr2,gr3,l,LInt,gr4,AH}
]
```

Below is the main *Mathematica 10* function used to generate the Vaidya-AdS$_4$ results. This function does the following: takes arguments r0,t,b,Col, where Col defines the line colour of the output figures. 1. Produce a inital solution Sol to calculate l/2 2. Produce SolL, i.e. the solution for v,r running from -l/2 to -x0 3. Returns in order: (1-3) plots of the surfaces in the rx,vx,rv planes, (4) ℓ, (5) Surface Area, (5) surface plot in x,v,r, (6) apparent horizon in x,v,r and (7) Surface in x,y,r. The plots produced from 3. may be reflected to give the full plots for $x \in [-\frac{\ell}{2}, \frac{\ell}{2}]$.

```
yL=1;
f[r0_,t_,b_,Col_]:=Module[{a,m0,Eqn1,Eqn2,r,x,v,rmax,xmax,x0,Sol,l,SolL
    ,gr1,gr2,gr3,LInt,dot,scal,gr4,temp1,AH,y,surplot,ab},
    a=1/3;
    m0=1;
    m[v_]:=m0(Tanh[v/a]+1)/2;
    Eqn1=r0^4(r[x]^2+2r'[x]v'[x]-(r[x]^2-m[v[x]]/r[x])v'[x]^2)-r[x]^
        6;

    Eqn2=3r[x]+r[x]^5/r0^4+(6r'[x]v'[x])/r[x]-3r[x]v'[x]^2-2v''[x]
    rmax=100;
    x0=1/3 r0^2/rmax^3;
    xmax=100;
    Sol=NDSolve[{Eqn1==0,Eqn2==0,r[x0]==rmax,v[x0]==t-1/rmax,v'[x0]=
        =-(rmax^2/r0^2)+b/r0^2},{r,v},{x,x0,xmax}];

    l=2*x/.Last[Quiet[FindMinimum[v[x]/.Sol,{x,x0,x0,xmax}]]];

    SolL=NDSolve[{Eqn1==0,Eqn2==0,r[-l/2]==rmax,v[-l/2]==t-1/rmax,v'
        [-l/2]==-(rmax^2/r0^2)+b/r0^2},{r,v},{x,-l/2,-x0},"Extrapol
        ationHandler"->{Indeterminate &}];

    gr1=Plot[{Evaluate[r[x]/.SolL],Evaluate[m[v[x]]^(1/3)/.SolL]},{x
        ,-l/2,l/2},PlotStyle->{Col,{Dashed,Black}},PlotRange->All];

    gr2=Plot[Evaluate[v[x]/.SolL],{x,-l/2,l/2},PlotStyle->{Col},Plot
        Range->All];

    gr3=ParametricPlot[{Evaluate[{v[x],r[x]}/.SolL],Evaluate[{v[x],m
        [v[x]]^(1/3)}/.SolL]},{x,-l/2,-x0},AspectRatio->1/GoldenRati
        o,PlotRange->All,PlotStyle->{Col,{Black,Dashed}}];

    AInt=yL2/r0^2*(NIntegrate[r[x]^4/.SolL,{x,-l/2,-x0}])-yL2rmax;

    gr4=ParametricPlot3D[Evaluate[{x,v[x],r[x]}/.SolL],{x,-(l/2),-x0
        },PlotRange->All,PlotStyle->Col];

```

```
    AH=ParametricPlot3D[Evaluate[{y,v[x],m[v[x]]^(1/3)}/.SolL],{x,-(
        1/2),-x0},{y,-(1/2),1/2},PlotRange->All,PlotStyle->{LightBlue
        ,Opacity[0.5]}];

    ab=ParametricPlot3D[Evaluate[{y,x,r[x]}/.SolL],{x,-(1/2),-x0},{y
        ,0,yL},PlotRange->All,PlotStyle->None]  ;

    surplot=Show[{ab},{ab}/.L_Line:>{GeometricTransformation[L,
    ReflectionTransform[{0,1,0}]]},PlotRange->{{0,yL},{-(1/2),1
    /2},{0,4}}];
{gr1,gr2,gr3,l,AInt,gr4,AH,surplot}
]
```

Bibliography

[1] Javier Abajo-Arrastia, Joao Aparicio, and Esperanza Lopez. Holographic Evolution of Entanglement Entropy. *JHEP*, 1011:149, 2010. doi: 10.1007/JHEP11(2010)149.

[2] Tameem Albash and Clifford V. Johnson. Holographic Entanglement Entropy and Renormalization Group Flow. *JHEP*, 1202:095, 2012. doi: 10.1007/JHEP02(2012)095.

[3] Vijay Balasubramanian and Per Kraus. A Stress tensor for Anti-de Sitter gravity. *Commun.Math.Phys.*, 208:413–428, 1999. doi: 10.1007/s002200050764. URL `http://arxiv.org/abs/hep-th/9902121`.

[4] Maximo Banados, Claudio Teitelboim, and Jorge Zanelli. The Black hole in three-dimensional space-time. *Phys.Rev.Lett.*, 69:1849–1851, 1992. doi: 10.1103/PhysRevLett.69.1849.

[5] K. Bautier, F. Englert, M. Rooman, and P. Spindel. The Fefferman-Graham ambiguity and AdS black holes. *Phys.Lett.*, B479:291–298, 2000. doi: 10.1016/S0370-2693(00)00339-7.

[6] Jacob D. Bekenstein. Black holes and entropy. *Phys. Rev. D*, 7:2333–2346, Apr 1973. doi: 10.1103/PhysRevD.7.2333. URL `http://link.aps.org/doi/10.1103/PhysRevD.7.2333`.

[7] Ingemar Bengtsson and Jose M.M. Senovilla. A Note on trapped Surfaces in the Vaidya Solution. *Phys.Rev.*, D79:024027, 2009. doi: 10.1103/PhysRevD.79.024027.

[8] Ivan Booth. Black hole boundaries. *Can.J.Phys.*, 83:1073–1099, 2005. doi: 10.1139/p05-063. URL `http://arxiv.org/abs/gr-qc/0508107`.

[9] J. David Brown and M. Henneaux. Central Charges in the Canonical Realization of Asymptotic Symmetries: An Example from Three-Dimensional Gravity. *Commun.Math.Phys.*, 104:207–226, 1986. doi: 10.1007/BF01211590.

[10] P. Calabrese and J. Cardy. Evolution of entanglement entropy in one-dimensional systems. *Journal of Statistical Mechanics: Theory and Experiment*, 4:10, April 2005. doi: 10.1088/1742-5468/2005/04/P04010.

[11] Pasquale Calabrese and John L. Cardy. Entanglement entropy and quantum field theory. *J.Stat.Mech.*, 0406:P06002, 2004. doi: 10.1088/1742-5468/2004/06/P06002. URL `http://arxiv.org/abs/hep-th/0405152`.

[12] Steven Carlip. Lectures on (2+1) dimensional gravity. *J.Korean Phys.Soc.*, 28: S447–S467, 1995. URL http://arxiv.org/abs/gr-qc/9503024.

[13] Steven Carlip. What we don't know about BTZ black hole entropy. *Class.Quant.Grav.*, 15:3609–3625, 1998. doi: 10.1088/0264-9381/15/11/020.

[14] Sebastian de Haro, Sergey N. Solodukhin, and Kostas Skenderis. Holographic reconstruction of space-time and renormalization in the AdS / CFT correspondence. *Commun.Math.Phys.*, 217:595–622, 2001. doi: 10.1007/s002200100381.

[15] C. Fefferman and C. R. Graham. The ambient metric. *ArXiv e-prints*, October 2007.

[16] Charles Fefferman and C.Robin Graham. Conformal invariants. Élie Cartan et les mathématiques d'aujourd'hui, The mathematical heritage of Élie Cartan, Sémin. Lyon 1984, Astérisque, No.Hors Sér. 1985, 95-116 (1985)., 1985.

[17] Willy Fischler, Arnab Kundu, and Sandipan Kundu. Holographic Mutual Information at Finite Temperature. *Phys.Rev.*, D87(12):126012, 2013. doi: 10.1103/PhysRevD.87.126012. URL http://arxiv.org/abs/1212.4764.

[18] S. W. Hawking. Particle creation by black holes. *Comm. Math. Phys.*, 43(3): 199–220, 1975. URL http://projecteuclid.org/euclid.cmp/1103899181.

[19] S.W. Hawking and Don N. Page. Thermodynamics of Black Holes in anti-De Sitter Space. *Commun.Math.Phys.*, 87:577, 1983. doi: 10.1007/BF01208266.

[20] Matthew Headrick and Tadashi Takayanagi. Holographic proof of the strong subadditivity of entanglement entropy. *Phys. Rev. D*, 76:106013, Nov 2007. doi: 10.1103/PhysRevD.76.106013. URL http://link.aps.org/doi/10.1103/PhysRevD.76.106013.

[21] Christoph Holzhey, Finn Larsen, and Frank Wilczek. Geometric and renormalized entropy in conformal field theory. *Nucl.Phys.*, B424:443–467, 1994. doi: 10.1016/0550-3213(94)90402-2. URL http://arxiv.org/abs/hep-th/9403108.

[22] Veronika E. Hubeny, Mukund Rangamani, and Tadashi Takayanagi. A Covariant holographic entanglement entropy proposal. *JHEP*, 0707:062, 2007. doi: 10.1088/1126-6708/2007/07/062.

[23] S.V. Ketov. Conformal field theory. 1995.

[24] Igor R. Klebanov, David Kutasov, and Arvind Murugan. Entanglement as a probe of confinement. *Nucl.Phys.*, B796:274–293, 2008. doi: 10.1016/j.nuclphysb.2007.12.017.

[25] Hong Liu and S. Josephine Suh. Entanglement growth during thermalization in holographic systems. *Phys. Rev. D*, 89:066012, Mar 2014. doi: 10.1103/PhysRevD.89.066012. URL http://link.aps.org/doi/10.1103/PhysRevD.89.066012.

[26] Juan Martin Maldacena. The Large N limit of superconformal field theories and supergravity. *Int.J.Theor.Phys.*, 38:1113–1133, 1999. doi: 10.1023/A:1026654312961.

[27] Samir D. Mathur. Black holes and holography. *J.Phys.Conf.Ser.*, 405:012005, 2012. doi: 10.1088/1742-6596/405/1/012005.

[28] N.E. Mavromatos. Eluding the no hair conjecture for black holes. 1995.

[29] Tatsuma Nishioka, Shinsei Ryu, and Tadashi Takayanagi. Holographic Entanglement Entropy: An Overview. *J.Phys.*, A42:504008, 2009. doi: 10.1088/1751-8113/42/50/504008.

[30] Shinsei Ryu and Tadashi Takayanagi. Holographic derivation of entanglement entropy from AdS/CFT. *Phys.Rev.Lett.*, 96:181602, 2006. doi: 10.1103/PhysRevLett.96.181602.

[31] Shinsei Ryu and Tadashi Takayanagi. Aspects of Holographic Entanglement Entropy. *JHEP*, 0608:045, 2006. doi: 10.1088/1126-6708/2006/08/045.

[32] Andrew Strominger. Black hole entropy from near horizon microstates. *JHEP*, 9802:009, 1998. doi: 10.1088/1126-6708/1998/02/009.

[33] N. Tetradis. Entropy from AdS(3)/CFT(2). *JHEP*, 1202:054, 2012. doi: 10.1007/JHEP02(2012)054.

[34] Edward Witten. Anti-de Sitter space and holography. *Adv.Theor.Math.Phys.*, 2:253–291, 1998.

[35] Edward Witten. Anti-de Sitter space, thermal phase transition, and confinement in gauge theories. *Adv.Theor.Math.Phys.*, 2:505–532, 1998. URL `http://arxiv.org/abs/hep-th/9803131`.

[36] Edward Witten. Three-Dimensional Gravity Revisited. 2007. URL `http://arxiv.org/abs/0706.3359`.

[37] A. Zaffaroni. Introduction to the AdS-CFT correspondence. *Class.Quant.Grav.*, 17:3571–3597, 2000. doi: 10.1088/0264-9381/17/17/306.